TKK Dissertations 82
Espoo 2007

# IMPROVING THE BIOMIMETIC PROPERTIES OF LIQUID/LIQUID INTERFACES: ELECTROCHEMICAL AND PHYSICOCHEMICAL CHARACTERISATION

Doctoral Dissertation

**Hélder A. Santos**

**Helsinki University of Technology**
**Department of Chemical Technology**
**Laboratory of Physical Chemistry and Electrochemistry**

TKK Dissertations 82
Espoo 2007

# IMPROVING THE BIOMIMETIC PROPERTIES OF LIQUID/LIQUID INTERFACES: ELECTROCHEMICAL AND PHYSICOCHEMICAL CHARACTERISATION

Doctoral Dissertation

**Hélder A. Santos**

Dissertation for the degree of Doctor of Science in Technology to be presented with due permission of the Department of Chemical Technology for public examination and debate in Auditorium KE2 at Helsinki University of Technology (Espoo, Finland) on the 28th of September, 2007, at 1 pm.

**Helsinki University of Technology**
**Department of Chemical Technology**
**Laboratory of Physical Chemistry and Electrochemistry**

**Teknillinen korkeakoulu**
**Kemian tekniikan osasto**
**Fysikaalisen kemian ja sähkökemian laboratorio**

Distribution:
Helsinki University of Technology
Department of Chemical Technology
Laboratory of Physical Chemistry and Electrochemistry
P.O. Box 6100
FI - 02015 TKK
FINLAND
URL: http://www.tkk.fi/Units/PhysicalChemistry/
Tel. +358-9-451 2579
Fax +358-9-451 2580
E-mail: helder.santos@tkk.fi



ISBN 978-951-22-8888-5
ISBN 978-951-22-8889-2 (PDF)
ISSN 1795-2239
ISSN 1795-4584 (PDF)
URL: http://lib.tkk.fi/Diss/2007/isbn9789512288892/

TKK-DISS-2326

Picaset Oy
Helsinki 2007

| HELSINKI UNIVERSITY OF TECHNOLOGY<br>P. O. BOX 1000, FI-02015 TKK<br>http://www.tkk.fi | ABSTRACT OF DOCTORAL DISSERTATION |
|---|---|

Author Hélder A. Santos

Name of the dissertation

Improving the Biomimetic Properties of Liquid/Liquid Interfaces: Electrochemical and Physicochemical Characterisation

| Date of manuscript March 22, 2007 | Date of the dissertation September 28, 2007 |
|---|---|
| ☐ Monograph | ☒ Article dissertation (summary + original articles) |

| | |
|---|---|
| Department | Department of Chemical Technology |
| Laboratory | Laboratory of Physical Chemistry and Electrochemistry |
| Field of research | Physical Chemistry and Electrochemistry |
| Opponent(s) | Dr. Robert Dryfe (University of Manchester, England) |
| Supervisor | Professor Kyösti Kontturi |
| (Instructor) | Docent Dr. Lasse Murtomäki |

Abstract

This thesis addresses the electrochemical and physicochemical characterisation of the interactions between modified phospholipid monolayers and other model membrane components, polysaccharides and proteins. Also, the assembly of metallic nanoparticles (NPs) on their surface at the polarisable liquid/liquid interfaces is studied. The thesis comprises six original publications and an introductory background to the relevant literature.

In the literature part, relevant background concerning the structure, composition and properties of biological membranes as well as model membranes is briefly reviewed. Classification of gramicidin (gA) ion-channels, glycosaminoglycans (GAGs), in particular dextran sulfate (DS), and glucose oxidase (GOx), with respect to their structure, properties and interaction with lipids is presented. Monolayers at soft interfaces, such as air/liquid and liquid/liquid interfaces, as well as the theory associated with them are also reviewed. Finally, a brief description of the NPs and their characteristics, and isothermal titration calorimetric properties is given.

In the latter part of the thesis, the essential results of the presented publications are summarised and discussed. The thesis introduces an approach to: (i) modify a phospholipid monolayer at a liquid/liquid interface with DS using calcium bridges between DS and the monolayer; (ii) construct polyelectrolyte/gold NP multilayers anchored to a lipid monolayer; (iii) prepare and characterise DS-modified ruthenium NPs, and to study their influence on drug transfer; (iv) study the influence of the peptide gA or enzyme GOx on the lipid layer as well as on the drug permeability; and (v) study the binding mechanism between drug and GAG molecules. Finally, the main conclusions and future perspectives are assessed.

All the studies presented in this thesis involved the combination of ac and dc electrochemical techniques, such as ac impedance/voltammetry and cyclic voltammetry, spectroscopic techniques such as FTIR and fluorescence, and surface (TEM) and calorimetric techniques. Furthermore, the capacitance curves were successfully explained and interpreted with theoretical models, in order to get a closer insight on the ion transfer and membrane interactions for each studied system. It is highlighted that electrochemistry can provide useful information on phenomena taking place at the membrane surface.

Keywords Liquid/liquid interface, phospholipid monolayers, dextran sulfate, capacitance, electrochemistry

| | |
|---|---|
| ISBN (printed) 978-951-22-8888-5 | ISSN (printed) 1795-2239 |
| ISBN (pdf) 978-951-22-8889-2 | ISSN (pdf) 1795-4584 |
| ISBN (others) | Number of pages 110 p. + publications 72 p. |

Publisher Helsinki University of Technology, Laboratory of Physical Chemistry and Electrochemistry

Print distribution Helsinki University of Technology, Laboratory of Physical Chemistry and Electrochemistry

☒ The dissertation can be read at http://lib.tkk.fi/Diss/2007/isbn9789512288892/

| TEKNILLINEN KORKEAKOULU<br>PL 1000, 02015 TKK<br>http://www.tkk.fi | VÄITÖSKIRJAN TIIVISTELMÄ |
|---|---|

Tekijä Hélder A. Santos

Väitöskirjan nimi

Parannettu Biomembraanimalli Neste-Neste –Rajapinnalla: Sähkökemiallinen ja Fysikokemiallinen Karakterisointi

| Käsikirjoituksen jättämispäivämäärä 22.3.2007 | Väitöstilaisuuden ajankohta 28.9.2007 |
|---|---|
| ☐ Monografia | ☒ Yhdistelmäväitöskirja (yhteenveto + erillisartikkelit) |

| | |
|---|---|
| Osasto | Kemian tekniikan osasto |
| Laboratorio | Fysikaalisen kemian ja sähkökemian laboratorio |
| Tutkimusala | Fysikaalisen kemian ja sähkökemian |
| Vastaväittäjä(t) | Tohtori Robert Dryfe (Manchesterin Yliopisto, Englanti) |
| Työn valvoja | Professori Kyösti Kontturi |
| (Työn ohjaaja) | Opettava tutkija Lasse Murtomäki |

Tiivistelmä

Väitöskirja käsittelee biomembraanimallia, joka muodostettiin fosfolipidiyksikerroksesta ja sitä modifioivista polysakkarideista ja proteiineista. Lipidikerroksen ja muiden membraanikomponenttien välisiä vuorovaikutuksia karakterisoitiin fysikokemiallisin ja erityisesti sähkökemiallisin menetelmin. Myös metallinanopartikkelien vuorovaikutusta membraanimallin kanssa tarkasteltiin käyttäen hyväksi polarisoituvaa neste-neste –rajapintaa membraanimallin rakentamiseksi.

Kirjallisuusosassa luodaan katsaus biologisten membraanien ja membraanimallin rakenteeseen, koostumukseen ja ominaisuuksiin. Gramisidiini A -ionikanavat (gA), glykosaminoglykaanit (GAG) - erityisesti dekstraanisulfaatit (DS) - sekä glukoosioksidaasit (GOx) luokitellaan niiden rakenteen, ominaisuuksien ja lipidivuorovaikutusten mukaan. Pehmeille rajapinnoille, kuten ilma-vesi - ja öljy-vesi -rajapinnoille rakennettujen lipidiyksikerrosten teoria ja työn kannalta relevantti tähän astinen kokeellinen aineisto esitellään lyhyesti. Työssä käytettyjen nanopartikkelien valmistus ja karakterisointi sekä isotermisen titrauskalorimetrian soveltaminen kuvataan lyhyesti.

Työn kokeellisessa osassa erillisjulkaisujen keskeiset tulokset on koottu yhteen. Väitöskirja lähestyy erityisesti seuraavia membraanimallin aspekteja: (i) fosfolipidikerroksen modifiointi liittämällä siihen DS:a $Ca^{2+}$-siltojen kautta; (ii) kultananopartikkeli-polyelektrolyytti -monikerrosten rakentaminen lipidikerroksen päälle; (iii) polyelektrolyytillä päällystettyjen Ru-nanopartikkelien valmistus, karakterisointi ja vaikutus lääkeaineiden läpäisyyn lipidikerroksen läpi; (iv) gA:n ja GOx:n vuorovaikutus lipidikerroksen kanssa ja vaikutus lääkeaineiden läpäisyyn; (v) lääkeaineiden sitoutumismekanismi GAG:iin. Lopuksi esitetellään tuloksista tehdyt johtopäätökset ja tulevaisuudennäkymät.

Työssä käytetyt kokeelliset menetelmät käsittävät tasa- ja vaihtovirrallisia mittauksia, FTIR- ja fluoresenssispektroskopiaa, TEM-kuvauksia ja kalorimetrisiä mittauksia. Sähkökemiallisilla mittauksilla saadut kapasitanssikäyrät sovitettiin elektrostaattiseen malliin, jonka avulla voitiin selittää kapasitanssin potentiaaliriippuvuus varsin hyvin. Työ osoittaa, että sähkökemiallisilla menetelmillä voidaan lähestyä biomembraanissa tapahtuvia prosesseja, jotka muuten ovat vaikeasti havainnoitavissa.

| Asiasanat | Neste-neste –rajapinta, fosfolipidiyksikerros, dekstraanisulfaatti, kapasitanssi, sähkökemia | |
|---|---|---|
| ISBN (painettu) | 978-951-22-8888-5 | ISSN (painettu) 1795-2239 |
| ISBN (pdf) | 978-951-22-8889-2 | ISSN (pdf) 1795-4584 |
| ISBN (muut) | | Sivumäärä 110 s. + julkaisut 72 s. |
| Julkaisija | Teknillinen korkeakoulu, Fysikaalisen kemian ja sähkökemian laboratorio | |
| Painetun väitöskirjan jakelu | Teknillinen korkeakoulu, Fysikaalisen kemian ja sähkökemian laboratorio | |

☒ Luettavissa verkossa osoitteessa http://lib.tkk.fi/Diss/2007/isbn9789512288892/

*Dedicated to the memory of my Father.*

*To my family for all their encouragement* ♣

# Preface

The present work was carried out at the Laboratory of Physical Chemistry and Electrochemistry, Helsinki University of Technology, Finland, from October 2003 to March 2007.

First and foremost, I would like to express my sincere gratitude to my supervisor, Professor Kyösti Kontturi, for providing me with the chance to study and work in his group. It has been a privilege to work under his inspiring guidance, advice and encouragement.

Also, I am very grateful to my instructor, Docent Dr. Lasse Murtomäki, for sharing his experience in the field of physical chemistry and electrochemistry, and for his helpful discussions and comments during the past three years.

I would like to give special thanks to the co-authors of the original publications of this thesis: Drs. Vladimir García-Morales and Mariana Chirea; Lics.Sc. (Tech.) Robbert-Jan Roozeman and Sanna Carlsson; M.Sc. Elisabete S. Ferreira and Mrs. Elisa J. Pereira; and Professors José A. Manzanares, Carlos M. Pereira, and Fernando Silva, for fruitful discussions and collaboration. Dr. Timo Laaksonen is also acknowledged for transmission electron microscopy of synthesized particles.

Dr. Annika Mälkiä is also acknowledged for helping me, in the very beginning of this thesis, with the setup of both Langmuir–Blodgett and electrochemical techniques. I am also grateful to Dr. Bernadette Quinn for proof-reading this thesis.

My sincere thanks also to Docent Dr. Leena Peltonen, from Division of Pharmaceutical Technology, University of Helsinki, and Dr. Frédéric Reymond, from DiagnoSwiss S.A. (Switzerland) for pre-reviewing this thesis and for their valuable comments.

In addition, my sincere thanks to friends, past and present research colleagues, and permanent staff within the Laboratory of Physical Chemistry and Electrochemistry, with whom I have had the pleasure to work during these years.

I further thank to all the participants within the SUSANA network, for friendship, scientific discussions, sharing their knowledge on nanoscience, and for all the

unforgettable moments spent together. This experience has been enriching.

Finally, my warmest thanks go to my family, especially to my parents, Dina and Serafim, and to my grandmother, Maria, for their everlasting support, encouragement and love; and to Marjo, for sharing her life with me, all her support, never-ending enthusiasm, optimism, and for bringing joy to my life. I am also deeply thankful to Marjo's family for all their friendship and support. I dedicate this thesis to all of you.

Financial support from European Union under the research and training network SUSANA ("Supramolecular Self-Assembly of Interfacial Nanostructures", contract number HPRN-CT-2002-00185), Finish Ministry of Education, Academy of Finland, and ESPOM (Electrochemical Science and Technology of Polymers and Membranes including Biomembranes) graduate school is also gratefully acknowledged.

Espoo, March 2007

Hélder A. Santos

# Table of Contents

# List of Publications

This thesis consists of an overview of the following publications which are referred to in the text by their Roman numerals.

**I** Hélder A. Santos, Vladimir García-Morales, Robbert-Jan Roozeman, José A. Manzanares, and Kyösti Kontturi, Interfacial Interaction Between Dextran Sulfate And Lipid Monolayers: An Electrochemical Study, *Langmuir* **2005**, *21*, 5475–5484.

**II** Hélder A. Santos, Mariana Chirea, Vladimir García-Morales, Fernando Silva, José A. Manzanares, and Kyösti Kontturi, Electrochemical Study Of Interfacial Composite Nanostructures: Polyelectrolyte/Gold Nanoparticle Multilayers Assembled On Phospholipid/Dextran Sulfate Monolayers At A Liquid–Liquid Interface, *J. Phys. Chem. B* **2005**, *109*, 20105–20114.

**III** Hélder A. Santos, Vladimir García-Morales, Lasse Murtomäki, José A. Manzanares, and Kyösti Kontturi, Preparation Of Nanostructures Composed Of Dextran Sulfate/Ruthenium Nanoparticles And Their Interaction With Phospholipid Monolayers At A Liquid–Liquid Interface, *J. Electroanal. Chem.* **2007**, *599*, 194–202.

**IV** Hélder A. Santos, Sanna Carlsson, Lasse Murtomäki, and Kyösti Kontturi, Effect Of Gramicidin On Phospholipid-Modified Monolayers And On Ion Transfer At A Liquid–Liquid Interface, *ChemPhysChem* **2007**, *8*, 913–920.

**V** Hélder A. Santos, José A. Manzanares, Lasse Murtomäki, and Kyösti Kontturi, Thermodynamic Analysis Of Binding Between Drugs And Glycosaminoglycans By Isothermal Titration Calorimetry And Fluorescence Spectroscopy, *Eur. J. Pharmaceut. Sci.* **2007**, *in press* (doi:10.1016/j.ejps.2007.06.003).

**VI** Hélder A. Santos, Elisabete S. Ferreira, Elisa J. Pereira, Carlos. M. Pereira, Kyösti Kontturi, and Fernando Silva, Adsorption–Penetration

Studies Of Glucose Oxidase Into Phospholipid Monolayers At 1,2–Dichloroethane/Water Interface, *ChemPhysChem* **2007**, *8*, 1540–1547.

# Statement of the Author's Contribution in the Listed Publications

Hélder A. Santos has actively taken part in planning, interpretation of all results, writing the papers, and was the principal author of all papers included in this thesis. He has planned and performed all the experimental work in all papers, I–VI. In papers I–III, the theoretical model used to interpret the capacitance results was done jointly with V. García-Morales, and in the case of paper I, with R.-J. Roozeman concerning the FTIR part. The theoretical work included in paper IV was done jointly with S. Carlsson, and that included in paper VI was done by the author.

Espoo, March 2007

Professor Kyösti Kontturi

# 1 Introduction

*"Exploratory research is really like working in a fog. You don't know where you're going. You're just groping. Then people learn about it afterwards and think how straightforward it was."*

*-Francis Crick*

The study of electrochemical processes at the interface between two immiscible electrolytes (ITIES) has become a very active area of research in contemporary electrochemistry. Its continuing interest is due to the applicability of these systems in many areas in chemistry and biology, such as charge transfer, electroanalysis, drug delivery and membrane biophysics.

Biological membranes play an important role in both the structure and function of all cells [1], and therefore simple models of membrane function are of great importance. Models can be improved by the incorporation of biomolecules in well-defined structures such as phospholipid monolayers [2]. The study of phospholipid monolayers is of great interest, because the monolayer is generally considered to represent half a biological membrane, which can be used to study specific molecular interactions, for example, between phospholipids, and between phospholipids and proteins or carbohydrates [3]. Theses compounds are also convenient for designing artificial systems with biological functions, such as biosensors and drug delivery devices [4]. The interaction of polyelectrolytes and nanoparticles (NPs) with charged surfaces has also been a hot topic in the literature, and plays an important role in colloid chemistry. It is the basis for numerous technical applications in fields such as biochemistry and electrochemistry, for example, in separation membranes, sensor materials and biosensors, as well as in delivery processes or devices [4].

Therefore, the aim of the present work was to modify the phospholipid monolayer at a liquid/liquid interface, and improve its applicability as a biomimetic membrane model. This was achieved by assembling anionic polyelectrolytes (such as dextran sulfate) on the polar phospholipid headgroup to resemble the glycosaminoglycan (GAG) network of the biological cell membranes. The modified phospholipid mono-

layer can also serve as an anchor for polyelectrolyte/NP layers, which are important when studying drug release kinetics. For example, by preparing water-soluble NPs combined with charged polyelectrolytes, the stability of drugs or proteins and their controlled release properties can be improved.

The interactions between membrane components, such as GAGs, and drug molecules with amphiphilic properties have also been investigated by advanced techniques, such as isothermal titration calorimetry (ITC).

In the first part of this thesis, an overview of biological membranes as well as their composition and structural details is given. Special attention will be paid to phospholipids, peptides (gramicidin A (gA) channels), enzymes (glucose oxidase (GOx)), and polysaccharides (GAGs). Furthermore, model systems for biological membranes, in particular those involving liquid/liquid interfaces, will be addressed, focusing on their experimental and theoretical aspects. Subsequently, a brief introduction to NPs, their characterisation and electrochemical applications is presented. Finally, the thermodynamic parameters obtained by ITC as well as their application in the interpretation of biological binding processes are briefly discussed in the latter section. This general background will be helpful for the interpretation of the results presented in the second part of the thesis.

In the second part, the main results and conclusions of the published work included are presented and discussed. The applicability of the systems studied here at the liquid/liquid interface and the methodologies used are very promising and can provide fundamental tools and ideas for further research of some biological phenomena. For example, they could be used to improve and/or monitor the transport and drug delivery of biologically active macromolecules across biological surfaces.

# 2 Literature Review

## 2.1 Cellular membranes

The membranes in living cells play a central role in both the structure and function of all prokaryotic and eukaryotic, plant and animal cells. For example, they regulate recognition events and solute permeability. Living cells sense their environment as a stimulus and make responses to environmental changes for the maintenance of life.

In 1925, an important breakthrough occurred when Gorter and Grendel proposed, by analysing erythrocyte membranes using a Langmuir trough, that phospholipids were arranged in the form of a biomolecular leaflet, or a phospholipid bilayer [5]. After that, Singer and Nicolson [6] presented a fluid mosaic model of the cell membrane which showed the membrane as a fluid-like bilayer in which the proteins are able to move freely. They stated that mimicking the design of the functional structure of biological membranes was essential for the exploitation of a new active field of membrane science and technology. Thereafter, proteins and sugars have been included into biological models, making them more heterogeneous, non-randomly compartmentalised bilayer structures [3,7]. Recently, biological membranes have been proposed to be more "mosaic" than "fluid", due to their variable patchiness, thickness and a higher protein occupancy than was generally considered [8]. Model membrane studies have shown that the lipid environment has a major effect on recognition events taking place at the cell membrane as well as on the interaction between biomolecules [9, 10]. For example, as lipid chain length is increased, the lipid binding capacity to other molecules is decreased and affects the exposure of binding moieties. Additionally, many interactions at the cell membrane occur through polyvalent binding, which requires flexible interacting molecules.

### 2.1.1 Structure and composition

All biomembranes have the same basic phospholipid bilayer structure and certain common functions, but each type of cellular membrane has different biological activ-

ities which are determined by the proteins associated with the membrane: peripheral proteins, which do not interact with the hydrophobic core of the bilayer; and integral proteins, all or part of which penetrate or span the phospholipid bilayer (see Figure 2.1).

Lipids serve multiple purposes both in living organisms and in material applications. The most abundant lipid components in membranes are phospholipids. They are amphiphilic molecules (i.e. they have a hydrophobic phosphate-containing headgroup and a hydrophobic hydrocarbon chain connected to a glycerol via ester bonds). They include phosphatidylcholine (PC), phosphatidylethanolamine (PE), phosphatidylserine (PS), phosphatidylinositol (PI), sphingomyelin (SM), and a small fraction of other lipids, such as the two negative charges possessing cardiolipin [1]. Phospholipids are asymmetrically distributed between the inner and outer monolayer of plasma membrane. Neutral PC and SM are found mainly in the outer monolayer. PE and negatively charged PS, PI, and phosphatidic acid (PA) are primarily located in the inner cytosolic monolayer [11].

Another component of the cell membrane is cholesterol. It modifies the structure and dynamic properties of the membrane, by changing the packing properties within the bilayer [12], depending on the phase state and phospholipid composition of the bilayer as well as the cholesterol concentration. Cholesterol is mainly hydrocarbon in composition, but it has an amphiphilic nature because its hydroxyl group can interact with the water. Cholesterol is present especially in the plasma membrane of mammalian cells but is absent from most prokaryotic cells.

Carbohydrates are also found in many membranes, covalently bound either to proteins as constituents of glycoproteins or to lipids as constituents of glycolipids (see Figure 2.1). Bound carbohydrates increase the hydrophilic character of lipids and proteins, helping to stabilise the conformation of many membrane proteins. The proteins embedded in the lipid bilayer, lipids themselves, carbohydrates and cholesterol form a characteristic pattern with locally enriched lipids floating as domains on the membranes (Figure 2.1).

Phospholipid monolayers at air/liquid and liquid/liquid interfaces can be used

as models for the biological membranes due to the symmetry and similarity of the two monolayers.

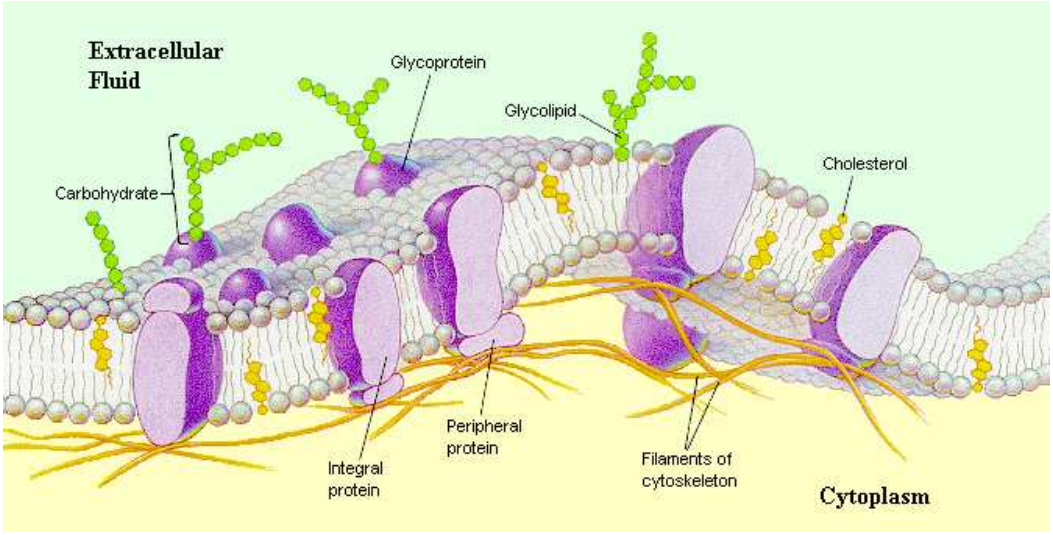


**Figure 2.1.** A schematic illustration of a typical biological membrane. Reproduced with permission from ref [13]. Copyright © (2005) Jones & Bartlett Publishers.

### 2.1.2 General properties of lipid bilayers

Lipids are linked to each other by weak forces rather than strong chemical bonds, such as van der Waals forces, hydrophobic interactions, and hydrogen-bonding, which make them very soft and flexible. These properties are necessary to carry out their principal functions.

Lipids can undergo various phase transitions, with phases reflecting different degrees of order, and exhibit so-called thermotropic phase behaviour (i.e., upon heating, the transitions from solid to liquid are not direct, but characterised instead by intermediate phases) [1, 14]. The most common phase transitions of lipids take place between fluid, gel (rippled, tilted, and untilted), and crystalline phases. The best characterised phase transition is that from the rippled gel-like to the fluid-like phase. The former phase represents an intermediate between the fluid and gel phases. It has recently been proposed by molecular dynamics simulations that the organization of lipid molecules in the lecithin ripple phase is gel-like and fully

interdigitated, while in the kink regions between the domains, lipids are highly disordered [15]. On the other hand, in the gel phase, the lipid acyl-chains are more ordered and the molecules are arranged in a regular structure. Any change in the phospholipid phase state will induce dramatic changes in the bilayer properties, such as compressibility modulus ($C_s^{-1}$) [2], surface potential, lateral packing and fluidity. Most of the biological membranes remain in the fluid phase state but other phases can exist within the membrane domain, as a result of the lipid/protein interactions [16]. The midpoint of the gel to crystalline phase transition for a given lipid is often referred as the melting temperature. Below the transition temperature, the hydrocarbon chains are tilted in a nearly all-*trans* conformation with contacts achieved by van der Walls forces, while above this temperature, the organisation of the chains become more disordered and adopts a *gauche* conformation which weakens van der Walls chain contacts. Consequently, the hydration and polar interactions of the phospholipid headgroups are also changed [17, 18].

Phospholipid and biological membranes have an internal lateral pressure that affects the stability, function, and assembly of the membrane, and is a result of the strong repulsions between the hydrocarbon chains that tend to expand the membrane and simultaneously squeeze out the hydrophilic headgroups in order to prevent exposure of the hydrocarbon tails to the solvent. In membranes, the internal lateral pressure is balanced by the hydrophobic effect (specifically its free energy density), while in lipid monolayers, lipid chains are free to escape from contact with water, and therefore internal lateral pressure must be balanced by an externally applied surface pressure [19]. Since the fluid membrane is self-assembled (unlike spread monolayer films), the total lateral pressure in the membrane is zero (or nearly zero), i.e. the bilayer will expand or contract in order to minimise the membrane free energy [20]. Properties of monolayers similar to those of bilayers are obtained at monolayer surface pressures of 30–35 mN/m, which corresponds to the range of equivalent pressure in the bilayer [19].

### 2.1.3 Model membranes

Over the past years, many model systems for biological membranes have been used. However, in this thesis, special attention is given to supported planar lipid membranes since they can provide a model system for investigating properties and functions of the cell membrane on a molecular level [3].

Supported phospholipid membranes can be formed with the Langmuir–Blodgett (LB) technique, which is frequently used to deposit thin films of amphiphilic molecules on solid supports. Molecules can be assembled with the LB technique in a well-defined arrangement and orientation. The packing density of the molecules at an air/liquid interface can be varied by a movable barrier and the surface pressure of the film spread can be measured by a Wilhelmy plate. Recording the surface pressure during the compression of the lipid monolayer can provide information on the monolayer phase properties and stability (see section 2.6 for further details).

The following sections will focus in detail on some of the components which are used in this thesis to model biological membranes, such gA, GAGs, and GOx.

## 2.2 Gramicidin ion-channels: structure and characterisation

In living systems, communication and interaction between cells and their environment is provided by, among others, membrane proteins. In this particular aspect, transmembrane ion channels which are usually narrow water-filled channels have an important role, providing pathways for the movement of charged particles across cell membranes, and mediating the interaction between the cell and its environment. They are also highly ion selective, playing a crucial role in cellular uptake of drugs that cross the membranes. For example, synthetic peptides can act as very efficient drug carriers with a very rapid internalisation process [21, 22].

Simple model membranes can therefore be improved by adding a model peptide to the lipid layer, enabling the study of ion transport in an environment similar to biological membranes. The study of the interactions between peptides, phospholipid

monolayers and bilayers has been of great interest [23–28]. The biological membrane structure and function can be disrupted by antimicrobial [23,24,26] and membrane-active [25] peptides, which seem to interact with the lipid matrix and not with the membrane proteins. However, the mechanism of action of these peptides is not yet fully understood.

There are different types of gramicidins, classified according to the position and number of residues in their chemical structure. The conducting channels are formed by the trans-bilayer dimerisation of nonconducting subunits, which are attached to the bilayer/solution interface through hydrogen bonds between the NH groups and the phospholipid backbone and water [29]. Gramicidin A (Figure 2.2) is the smallest transmembrane ion-channel and the most widely studied [29–31]. Gramicidin A is a highly hydrophobic membrane-active linear pentadecapeptide with a primary structure consisting of 15 alternating sequence of L- and D-amino acid residues and capped at its end with tryptophan subunits [29, 30]. Gramicidin A has also antibiotic properties and it is selective, allowing for the permeation of monovalent ions [32–34], such as potassium and sodium, and blocking divalent cations, such as calcium [35, 36]. In membrane-like environments, gA ion-channel structure is a head-to-head dimer of two right-handed single stranded $\beta$-helices with 6.3 residues ($\beta^{6.3}$) per turn [37–40], through the hydrogen bonding of the terminal formyl groups within the hydrocarbon environment [41]. Thus, in lipid bilayers, the side chain residues of the gA channel are in contact with the hydrophobic regions of the lipids and the carbonyls and amides face the hydrophilic pore of the peptide [37].

The phospholipid environment affects the gramicidin structure and sometimes the $\beta^{6.3}$ helix acts similarly to the channel lumen [28]. On the other hand, the incorporation of the peptide into lipid bilayer systems affects the lateral lipid organisation and domain size distribution [43]. In phospholipid monolayers, the four-tryptophan residues of the $\beta^{6.3}$ helices are oriented next to the C terminus and contact directly with the polar region groups of the membrane [44–47]. Tryptophan residues also mediate the interactions between the hydrophobic region of adjacent lipid molecules as well as cations inside the ion channel [48]. The functional gA channel is about 25

**Figure 2.2.** A schematic 3D-image of gA showing the tryptophan groups in each extremity of the dimer. Reprinted with permission from ref [42]. Copyright © (2002) American Chemical Society.

Å long, and its hydrophilic pore about 4 Å in diameter, containing a single water molecule wire comprised of seven to nine water molecules [49,50]. It has been shown that PCs and PEs affect differently the gating properties of gramicidin [51,52].

Studies of monolayers at the air/liquid interface have shown horizontal aggregation of gA molecules even at very low phospholipid/gA ratios [53], and a significant change in the dipole potential of phospholipid monolayers [54]. Furthermore, electrochemical impedance spectroscopy (EIS) has shown that the interaction between gA and phospholipid monolayers increases the surface roughness, introducing an extra capacitive element [55], and such interactions are also dependent on the gramicidin structure [28]. Isotherms of gA in the absence of lipid have shown a deflection point at low surface pressures [51], and this may be due to the irreversible dimerisation of gA [56]. This deflection point seems to disappear as the mole fraction of gA in the lipid monolayer is decreased below 0.5 [51], and dramatic changes in the gA orientation are then observed [56]. X-ray reflectivity measurements have shown a gramicidin film thickness on water of about 27 Å [57]. Using cyclic voltammetry and EIS, it has been demonstrated that the permeability of gramicidin channels to ion transport is dependent on the: (i) gramicidin concentration, (ii) applied poten-

tial across the membrane, and (iii) temperature. Polarisation modulation Fourier transform infrared (PM-FTIR) data has indicated a dependence of the peptide orientation on the applied surface pressure for mixed lipid/gramicidin monolayers [58], and PM infrared reflection absorption spectroscopy has suggested the presence of oriented water molecules between the bulk and the gramicidin monolayer [59].

A further characterisation of the monolayer can be achieved, by for example, transferring it onto a solid support. In this particular case, monolayer-covered mercury electrodes have been shown to be a feasible model membrane to study pore forming compounds [44, 60]. The transport mechanism and ion permeability through gramicidin channels have been described to resemble pore diffusion [44]. Ionophore antibiotic A23187 was observed to increase the permeability of the monolayer to $Cu^{2+}$ and $Cd^{2+}$ ions, by complexing the metal ion in the monolayer. This complex led to a conformational change in the monolayer and subsequent release of the ion at the electrode surface. Thallium (I) reduction has also been studied by several authors because it takes place at potentials at which the phospholipid film is impermeable, and thus the ion can only be reduced through the gramicidin half-channels [61–64]. However, many of these reports have focused mainly on the electron transfer mechanism.

Although pore forming molecules have been successfully incorporated in mercury-supported monolayers and despite the stability of the mercury/monolayer system, the mercury drop electrode method is mainly limited to electrochemical characterisation methods. Furthermore, production of toxic mercury waste and the incapability to study ion transfer makes this method less attractive.

## 2.3 Glycosaminoglycans and proteoglycans: structure, properties and classification

The glycoproteins of the cell membranes contain oligosaccharides attached to the protein either through so-called *O*-linkages (*O*–linked) or via glycosylaminyl linkages (*N*–linked) [65]. The core proteins are composed of proteoglycans (PGs), that con-

tain unbranched polysaccharides with long chains (usually $O$–linked) called GAGs or mucopolysaccharides. GAGs are attached to core proteins through a short polysaccharide linkage region (xylose-galactose-galactose-glucuronic acid). GAGs are a family of sulfated polysaccharides involved in a variety of different biological processes, such as neural development, tumour growth and metastasis, viral invasion and spinal cord injury [66–68]. They are composed of repeating disaccharide units of hexuronic acid and a hexosamine, both linked by $\beta$–1,3–glycosidic bonds. For example, GAGs modulate key signaling pathways essential for proper cell growth and angiogenesis [67], and have also been linked to the pathology of Alzheimer's disease [69]. They are highly anionic molecules due to the presence of the carboxylic and sulfate groups. Depending on the cell type and their role in the body, GAGs are major components in variable amounts in the extracellular matrices (ECMs) of many tissues, for example, vascular walls and connective tissues, but also inside and on the surface of cells [70]. GAGs adopt an extended conformation, attract cations and bind water. Hydrated GAG gels enable joints and tissues to adsorb large pressure changes [71].

The structure of different types of GAGs are shown in Figure 2.3. They include hyaluronan (HA, also called hyaluronic acid or hyaluronate), chondroitin sulfate (CS)/dermatan sulfate (DmS), heparan sulfate (HS)/heparin, and keratan sulfate (KS).

In the few past years, much attention has been paid to the study of GAGs, and in particular to its influence and/or interaction with the other components or compounds that exist or may reach the cell membrane. Polyanionic GAGs might bind to positively charged polymers and lipids, thereby affecting their mobility in tissue and/or their interaction with target cells. GAGs are structural and functional modulators of ECM and are, therefore, extremely important to the development and repair of the central nervous system [73]. Recent studies have shown that GAGs may carry out an important role in gene delivery systems [74, 75]. Cell membrane-associated GAGs mediate cellular entry of DNA complexes both *in vitro* [76] and *in vivo* [77], and may act as receptors for gene delivery complexes. On the other hand,

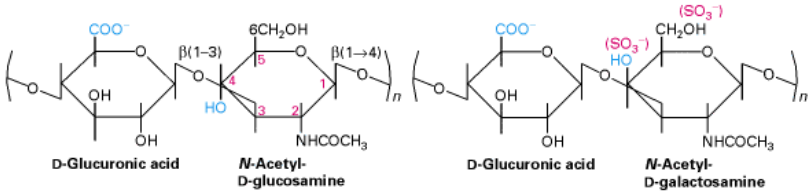


(a) HA




(b) CS

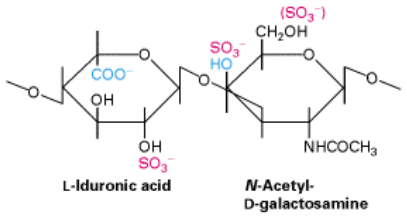


(c) DmS

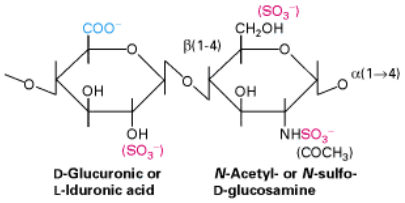


(d) HS/Heparin

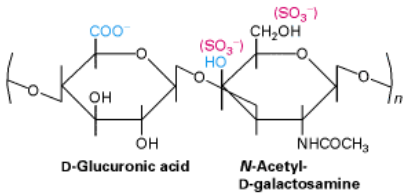


(e) KS

**Figure 2.3.** Structure of various GAGs, the polysaccharide components of PGs, and their repeating disaccharides units. The number ($n$) of disaccharides in a GAG chain can vary from 10 up to 50,000. The molecular weight can vary from 1 kDa up to $10^7$ kDa. Reproduced with permission from ref [72]. Copyright © (2000) W.H. Freeman Publisher.

interaction between extracellular GAGs and various complexes has been shown to decrease the gene transfer efficiency depending on the structure and charge densities of GAGs [74, 76].

## 2.4 Biological importance of dextran sulfate

In all the studies reported in this thesis involving lipid/GAG interactions, the negatively charged dextran sulfate (DS, Figure 2.4) was used as the model for GAGs. At neutral pH, DS is a highly negatively charged polyion similar to heparin with a partially branched carbohydrate backbone. Therefore, it is representative of the

carbohydrate moieties of GAG molecules and can be used instead of GAGs in several investigations. There has been an increasing interest in the study of the membrane-associated DS interactions because it was found that DS, together with calcium ions ($Ca^{2+}$), participate in numerous interactions with phospholipid films, carrying out an important role as an anti-atherosclerotic drug [78], an anti-HIV infection agent [79], and also as a carrier of drug molecules. It has been recently suggested that DS could be used to enhance the first step of protein transduction (a process by which genetic material is inserted into a cell using viruses as a carrier) due to electrostatic interactions between them and GAGs on the cell surface [80].

It has also been demonstrated that DS can be used to increase the gene transfer efficiency into cells by its incorporation into self-assembled polyethylenimine (PEI)–DNA/protein complexes [81, 82]. Thus, protein damage during drug formulation or cytotoxicity of PEI/DNA particles can be minimised as the amount of DS in the formulation increases.

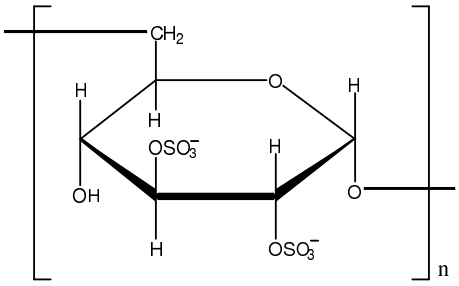


**Figure 2.4.** Schematic representation of the molecular structure of DS.

### 2.4.1 Interactions between DS/GAGs and lipoproteins

The surface of cells, viruses, and lipoproteins interact with a wide variety of ions, proteins, and other molecules in the aqueous medium. Pathological processes such as the adhesion of plasma low-density lipoproteins (LDLs) to components of the ECM of the connective tissue of the arterial walls are also related to such interactions. Contacts between LDLs and connective tissue are possible when the innermost cell layer of the arterial wall is damaged and GAGs of ECM are exposed to the blood-

stream. Interaction or association between polyelectrolytes and membrane surfaces leads to the development of arteriosclerosis [83, 84].

Associations between LDLs and GAGs have been studied for more than 40 years. In the very first studies, it was thought that the complex formation between DS and lipoproteins was caused by polar forces that involved mainly the phospholipids exposed at the surface rather than the protein moiety [85, 86]. However, the methods used in the early studies could not eliminate the role of the protein moiety from the DS/lipoprotein interaction.

Iverius [87] has studied the effect of the physiological pH and the ionic strength on the GAG/lipoprotein interactions, and found that they could be interpreted in terms of electrostatic binding between polyvalent anionic and cationic sites. The GAG charge density has also been shown to be a determining factor for the strength of the ionic bond. Thus, a stronger interaction was expected for GAGs containing iduronic acid than those containing glucuronic acid. Other studies have supported the idea that in the absence of divalent metals ions, the protein charged groups rather than the phospholipid charged groups, indeed play a major role in the DS/lipoprotein interactions [84].

*Effect of calcium ions on DS/lipoprotein interactions*

The addition of divalent metal ions was found to provide additional information on the charge characteristics of the lipoproteins on DS/lipoprotein interactions [88, 89]. In the absence of divalent metal ions, positively charged lipoprotein groups were the main factors responsible for the interaction. On the other hand, the addition of divalent metal ions led to the formation of insoluble complexes due to both positive and negative charges of lipoproteins. These findings confirmed the importance of the protein charged groups in GAG/lipoprotein interactions, rather than the phospholipid charged groups. Nevertheless, the additional adhesion forces were attributed to the phospholipid component of the LDLs [84, 89–91].

Charged phospholipid headgroups have also appeared to contribute to the elec-

trostatic interaction in the presence of divalent metal ions, such as $Ca^{2+}$, depending on the type of sulfated GAGs used, and on the concentration of the species in the system. For example, at millimolar $Ca^{2+}$ concentrations found in the extracellular space, precipitation of pure PC vesicles with GAGs could be achieved resulting in insoluble complexes, i.e. the inclusion of DS in liposomes resulted in liposome aggregation [88]. The formation of insoluble complexes with DS was attributed to the attractive forces generated by both the electrostatic interactions between the phospholipid choline nitrogen and sulfate groups of DS, and the cross-linking of the phosphate groups to the sulfate or phosphate groups of neighbouring phospholipids [88, 90]. For example, in precipitated lysolecithin micelles, a ratio of 2:1:3 for lipid/$Ca^{2+}$/DS complexes was found. These interactions are very important to understand certain mechanisms concerning the development of atherosclerosis.

The associations of GAGs with PCs is of great importance to the deposition of lipoproteins in the arterial intima [83]. An ionic interaction between the positively charged aminoacids of the lipoprotein and the negatively charged GAG molecules was presented as a possible explanation for GAG/PC associations [92], which was thought to be a key molecular process in atherogenesis [83, 93, 94].

Several other studies have concentrated on the interactions between liposomes and GAGs. $Ca^{2+}$ ions have been considered to be crucial to the binding between DS and neutral phospholipid liposomes [95]. Binding was shown to occur in the presence of $Ca^{2+}$, and in the presence of positively charged liposomes (vesicles), DS was bound without $Ca^{2+}$. The adsorption of DS leads to the aggregation of vesicles due to a bridging mechanism between adjacent liposomes as a result of two major factors: (i) the positive surface potential resulting from $Ca^{2+}$ or incorporation of positively charged molecules in vesicles, a prerequisite for the binding of the anionic DS; and (ii) the presence of high concentrations of DS.

In general, all the studies mentioned above have shown that the interaction of LDLs with anionic GAGs was a result of an electrostatic attraction between the GAG negatively charged sulfate groups and clusters of positively charged amino acids on the protein component of LDLs [96–98].

### 2.4.2 Calcium-mediated interaction between DS/GAGs and lipids

Following the conclusions of the previously described reports, it was confirmed by zeta potential measurements that the binding of GAG to PC was mediated by $Ca^{2+}$ ions [95, 99], and that the size of liposome/$Ca^{2+}$/GAG complexes increased with increasing GAG concentration until a saturation point was reached, after which complexes disaggregated [88,95]. The interaction between zwitterionic phospholipids and sulfated GAG mediated by $Ca^{2+}$ was considered to be rather strong, since pure PC liposomes and micelles formed large aggregates with GAG at physiological $Ca^{2+}$ concentrations (2–3 mM) [88, 95, 99].

Although the previous studies on PC/$Ca^{2+}$/GAG and LDL/$Ca^{2+}$/GAG complexes have provided new insight to understand the binding mechanism, they have mainly focused on the biophysical properties of the complexes as a whole, but little was known about the consequences of this association on the lipid packing in the monolayer as well as in the core of LDL particles. Fluorescence measurements have shown dehydration of the phospholipid surfaces caused by the $Ca^{2+}$-induced GAG binding, which would be responsible for the increase in the lipid phase transition temperature upon GAG binding [100].

Structural changes of phospholipid or LDLs in response to GAG association and the structure of the adsorbed layer itself in lipid/$Ca^{2+}$/GAG complexes have been investigated by nuclear magnetic resonance (NMR). This technique is very sensitive to lipid chain packing and the molecular area of phospholipids in the membrane. NMR has shown two major effects of the GAG/DS binding via $Ca^{2+}$ bridges: (i) a liquid-ordered phase was formed with reduction of the lateral diffusion rate of phospholipids in the monolayer of LDLs, and (ii) a minor reorientation of the phospholipid headgroup toward the membrane surfaces [101–103]. $Ca^{2+}$-mediated DS adsorption to PC surfaces was interpreted as a combination of two factors, a complex equilibrium between attractive forces, caused by $Ca^{2+}$ bridge formation between the phosphate of the lipid headgroups and the sulfate of the DS molecules, and repulsive electrostatic forces between adsorbed DS strands.

Longer-chain DSs have been observed to strongly influence the structure of

the phospholipid headgroup [102]. Depending on the amount of adsorbed DS, its association to phospholipids was found to occur in different structural ways: train-like, loop-like, and tail-like. Some $Ca^{2+}$ ions were bound to the DS sulfate groups and to the phospholipid phosphate group, whereas free $Ca^{2+}$ was accumulated near the surface of the double-layer, thus screening the DS negative charges. When the DS chain was partially desorbed from the lipid surface, it was held to lipids via $Ca^{2+}$ bridges by the remaining chain segments.

*Air/liquid studies of DS/lipid interactions*

Other techniques have been used to elucidate the interactions described in the previous section. For example, differential scanning calorimetry has demonstrated that the core lipids of LDL (cholesterylesters, triglycerides) form an isotropic fluid phase at body temperature, but after binding to GAG via $Ca^{2+}$, they form a liquid ordered state [103]. By studying the influence of $Ca^{2+}$-mediated GAG binding, the observed phase transition in the LDL core lipids was attributed to the changes in the lipid packing at a physiological $Ca^{2+}$ concentration. As a result, $Ca^{2+}$ bridges between the phospholipid polar headgroups and DS molecules were formed [104]. No evidence of penetration of DS to the hydrophobic region was observed, but the surface tension decreased by up to 3.5 mN/m. It was suggested that PC/$Ca^{2+}$/DS complexes with higher lipid packing were probably formed as indicated by a higher degree of lipid-chain ordering, extended tail conformation and decrease in the area per lipid molecule [100, 102, 104]. Interestingly, when the electrostatic interaction between DS and the phospholipid was modified by changing $Na^{+}$ and $Ca^{2+}$ concentrations, a maximal area reduction of 2.7 $Å^2$ per PC molecule, and an increase in the lipid main-phase transition temperature upon formation of PC/$Ca^{2+}$/DS complexes was observed. These results were in good agreement with those reported previously [101–103].

Since the molecular structure is of great relevance for physicochemical properties of the monolayers and membranes, the changes in the lipid monolayer coupled to DS in the presence of $Ca^{2+}$ were also studied at the air/liquid interface before

and after injection of DS to the subphase [105]. As a result of the DS binding to a non-charged phospholipid, an increase in the lateral lipid density was observed, with the isotherms shifted towards a more condensed state, showing that DS adsorbed directly at the monolayer. Applying grazing angle X-ray diffraction and ellipsometry techniques, it was also concluded that this system was more flexible than systems where the charged lipid monolayer was coupled to oppositely charged polyelectrolytes [106]. Furthermore, after DS binding to the lipid monolayer, the transition pressures and tilt angles were lowered, and the whole system appeared to be more flexible due to the bridging mechanism.

X-ray diffraction confirmed that the bridging mechanism provided an attractive force that caused the lipid surfaces to approach each other, and counterbalancing repulsive hydration, electrostatic, and steric forces [104, 107–109]. Using solid-state NMR, Huster et al. [110] studied the influence of DS binding on the lateral packing properties of cationic bilayer membranes in the absence of $Ca^{2+}$. In this case, it was concluded that the reduction observed in the lateral lipid packing density was caused by the membrane surface dehydration due to DS binding, which created attractive forces between bilayers. It was also shown that the repeated spacing of PC multilayers was reduced to 6–7 $Å^2$ due to PC/DS interaction in the presence of $Ca^{2+}$ [102, 104].

## 2.5 Glucose oxidase: characterisation and applications

Many cellular processes are catalysed by membrane-bound enzymes that can be found in each component/organelle of the cell. By being bound to a particular membrane or membrane region, the site of catalysis can be localised in the cell. There are numerous examples in which several enzymes that act sequentially are localised together in this manner, thus enhancing the overall reaction rate.

GOx is an enzyme that has attracted immense interest due to its applicability in biosensors for the determination of glucose in body fluids, as well as for removing glucose and oxygen from beverages and food products. The fact that GOx is easily

obtainable and robust, associated to its specific properties, makes it convenient to use as an initial model for exploring the reactivity of redox enzymes at interfaces [111].

GOx (Figure 2.5) is a dimeric globular glycoprotein of dimensions 60 × 52 × 77 $Å^3$, composed of two identical subunits, each of molecular weight of ca. 75 kDa, that are bound with disulfide bridges, salt linkages, and hydrogen bonds [112]. A considerable part of GOx hydrophobic side chains are located near the surface [113]. Its structure is composed of one redox coenzyme, flavin adenine dinucleotide (FAD), per monomer. The FAD is not covalently bound to the protein and can be released under denaturing conditions. FAD is a common component in biological redox reactions.

GOx has a diffusion coefficient of $4.94 \times 10^{-7}$ $cm^2$ $s^{-1}$ in 0.1 M NaCl [113]. According to photon correlation spectroscopy data, the average diameter of the native enzyme in solution is 76 Å at pH 7.4, the Stokes radius 43 Å with a frictional ratio of 1.21, and it appears as an elongated protein with rigid structure [114]. It has also been stated that each GOx monomer is a compact spheroid of dimensions 60 × 52 × 37 $Å^3$, presenting an isoelectric point of 4.44, and at pH 7, it is negatively charged with 11 charges [112].

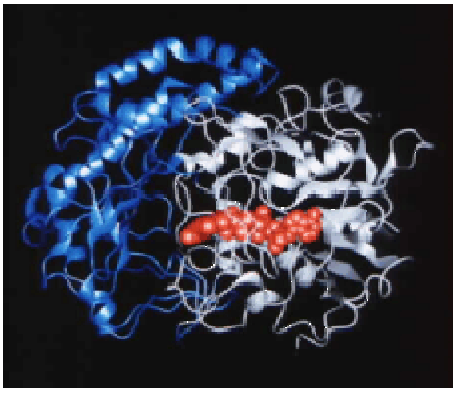

**Figure 2.5.** Subunit structure of GOx showing FAD (red space fill). Reproduced with permission from ref [115]. Copyright © Biological Sciences, University of Paisley, Scotland.

### 2.5.1 Interfacial interactions of glucose oxidase at air/liquid and liquid/liquid interfaces

The adsorption of GOx at both the ITIES and the air/water interface has been shown to be dependent on time, GOx concentration, and ionic strength [116]. Using capacitance measurements, Georganopoulou et al. [116] have shown an interaction between the adsorbed GOx and the hydrophobic cation in the organic phase. At the air/water interface, the adsorbed GOx seemed to dissociate into monomers at low salt concentrations, and retained its dimer structure at high salt concentrations. The adsorption mostly resulted in monolayers, with an effective thickness depending on the bulk concentration, due to deformation of GOx packing at the interface. The authors also reported that bilayers of GOx began to form at GOx concentrations $>$ 1 $\mu$M, with the formation of less densely packed layers on top of the first ones.

The interactions between lipid monolayers and GOx using LB and other techniques have also been described in the literature. Sun and co-workers [117] showed that the surface area per enzyme molecule at the air/water interface varied from 700 to 2200 Å$^2$, depending on the spreading conditions. In their work, films of GOx were spread at the air/water interface and transferred to Si or Pt substrates with the LB method. The subphase had a pH = 6 and consisted of 5 mM $BaCl_2$. Native enzyme gave LB films with very low activity and apparent thickness of 30 Å$^2$/layer. It was concluded that the protein had largely dissociated into monomers at the interface and that these monomers were adsorbed with the shortest axis parallel to the interface. By treating the enzyme with glutaraldehyde to cross-link the monomers before spreading on the interface, the authors also observed that the LB films retained a high glucose oxidation activity, which increased linearly with number of layers deposited. The apparent thickness in this case was 48 Å$^2$/layer. The results indicated that cross-linking with glutaraldehyde prevented dissociation of the enzyme upon adsorption.

Second-harmonic generation studies of GOx adsorption at the air/water interface, with aqueous solutions at high ionic strength ($I$ = 0.1 M, pH = 7), showed that the signal associated with GOx adsorbed at the air/water interface exhibited

a shoulder at 0.10 $\mu$M enzyme concentration and a maximum at 0.40 $\mu$M, subsequently decreasing for higher enzyme concentrations [118]. This was interpreted as an effect of protein/protein interactions, involving enzyme rearrangement and reorientation at the interface.

Rosilio et al. [119] reported GOx adsorption at the air/solution interface in the presence and absence of dibehenoyl-PC (DBPC) monolayers by monitoring the surface tension and surface potential. They proposed that the adsorption of GOx occurs by initial penetration into the lipid layer. The difference in adsorption in the presence and absence of the phospholipid layer was attributed to a possible GOx conformational change, due to hydrophobic interactions with the hydrocarbon chains of the lipid [120]. Following the described work, Baszkin et al. [114] investigated GOx incorporation into phospholipid and cholesterol monolayers. Two methods were used to monitor film compression: constant area, where successive addition of lipid aliquots decreases the area per molecule in steps, and in dynamic conditions, where lipid molecules are pushed by a barrier and confined to a small area. The lipid monolayer surface pressure decreased independently of the mode of film compression, and the surface pressure changes could be related to the rate of enzyme penetration (GOx and GOx modified by an ester of palmitic acid, *N*-hydroxysuccinimide) into PC, PE, PS, and cholesterol monolayers. The rate was dependent on the lipid nature and enzyme concentration. Modified GOx compared with GOx showed enhanced penetration capacity into all studied lipid and cholesterol monolayers. Using surface pressure vs time or surface density measurements, they realised that GOx adsorption into phospholipids was essentially due to the hydrophobic interaction between the phospholipid hydrocarbon chains and the penetrating enzyme.

Other studies [121] have shown that the presence of a double bond in the hydrophobic chains of dioleyl-PC favoured GOx adsorption, probably due to the fluidity of these monolayers and to the formation of hydrogen bonds between the two molecules. A more recent study [122] showed the effect of both lipid headgroup charge and aqueous subphase pH on GOx adsorption into DBPC and octadecylamine (ODA) monolayers. It was shown that the GOx adsorption into pure DBPC

monolayers essentially depends on the available area in a monolayer to hold adsorbing GOx molecules. In this case, the GOx penetration process into a monolayer occurs at high surface pressures. The authors stated that the enzyme penetration kinetics were dependent on the initial surface pressure of the spread monolayer, and that the addition of ODA to DBPC monolayers enhanced the GOx penetration. This was attributed to the strong attractive electrostatic interactions between the positively charged ODA and the negatively charged GOx.

## 2.6 Monolayer isotherms: phase properties

Monolayers are defined as monomolecular insoluble films on the surface of a liquid and were probably studied first by Benjamin Franklin [123]. Later, they became known as Langmuir monolayers due to the seminal work of Irving Langmuir [124] on monolayers at the air/liquid interface. Years later, Katherine Blodgett extended Langmuir's work by transferring the monolayer assemblies from the water surface to solid supports, forming so-called LB films [125]. Langmuir monolayers are mainly formed on the surface of water by amphiphilic molecules. Langmuir monolayers are of great interest because through them, phase transitions in two dimensions can be studied, with direct control of the temperature and surface pressure. They are also an excellent model for membrane biophysics, since a biological membrane can be considered as two weakly coupled monolayers.

It is well-known that at thermodynamic equilibrium, the surface tension, $\gamma$, of a planar interface can be related to the partial derivatives of the Gibbs free energy of the system, $G$, with respect to the area, $A$, of the surface by equation 2.1 [2]:

$$\gamma = \left(\frac{\partial G}{\partial A}\right)_{T,P,n_i} \tag{2.1}$$

The surface pressure $\pi$, the two-dimensional analogue of the hydrostatic pressure, is defined as the difference between the surface tension in the absence ($\gamma_0$) and presence ($\gamma$) of the amphiphile:

$$\pi = \gamma_0 - \gamma \tag{2.2}$$

The monolayer properties can be evaluated from the plots of $\pi$ vs $A$ at constant temperature, the so-called $\pi$–$A$ isotherms. Figure 2.6 shows an example of a generalised isotherm for a Langmuir monolayer. The monolayer can be also characterised by the compressibility modulus $C_s^{-1}$, according to equation 2.3 [126]:

$$C_s^{-1} = -\frac{1}{A}\left(\frac{\partial A}{\partial \pi}\right)_T \tag{2.3}$$

Different monolayer phase behaviour can be observed from the isotherms. A very dilute monolayer (with an area per molecule spanning hundreds of $\text{Å}^2$) is described as a two-dimensional gas. As $\pi$ increases (the area per molecule decreases), the monolayer advances to the liquid–expanded phase (LE). Here, as in the gas phase, no detectable X-ray diffraction signal is observed, because the heads of the molecules might be translationally disordered and the chains conformationally disordered [127]. Further monolayer compression gives rise to a transition from LE phase to a liquid–condensed (LC) phase. The plateau observed in this phase indicates a first-order transition, but is not completely horizontal in many systems, due to a phase coexistence [126], and due to the possible formation of small molecular aggregates or surface micelles [128, 129]. In the LC state, the monolayer is less compressible than in the LE state. Upon further compression, a kink (corresponding to a phase transition) can be observed in the isotherm, with the compressibility decreasing further after the kink. The two isotherm regions with different compressibilities are called "condensed" and "solid" states (here the monolayer hydrocarbon chains are aligned, in contrast with expanded states where the chains are conformationally disordered). X-ray diffraction studies have shown that the hydrocarbon chains are aligned parallel to each other in the isotherm: either tilted with respect to the water surface or perpendicular to it (untilted) [130]. In the tilted state, the monolayer is relatively easily compressible, and by decreasing the tilt angle, the surface area can be

decreased. Since the distance between close-packed vertical molecules determines the mean molecular area, the untilted state is less compressible. Continuing the compression will lead to monolayer collapse where the molecules can no longer pack more tightly, and hence are squeezed out of the monolayer. At this point, the surface pressure decreases as the surface area decreases.

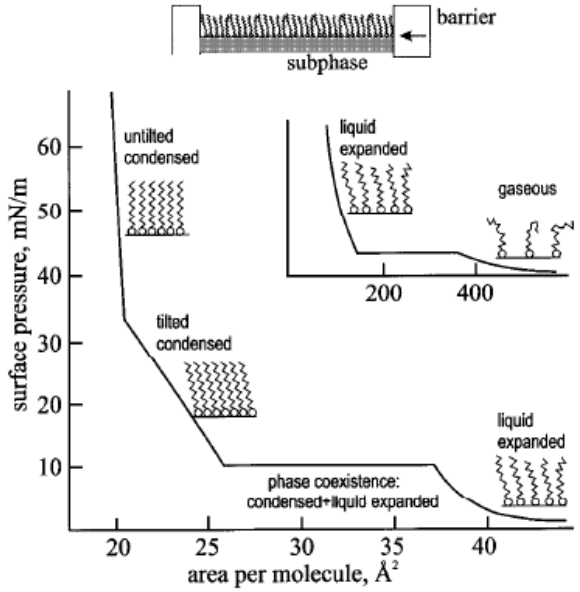


**Figure 2.6.** Representation of a Langmuir trough (top) and a Langmuir isotherm (bottom). Reprinted with permission from ref [130]. Copyright © (1999) American Physical Society.

The advantage of using Langmuir monolayers instead of bilayers is that from the isotherms, information on the intermolecular interactions can be extracted that is not accessible directly from bilayers because they are tension-free in their natural state [19]. Most interest has been focused on the area per molecule in the monolayers LE state, because under these conditions, at $\pi \approx 34$ mN/m (at 20 °C), the chain orientation and packing is likely to be similar to that in fluid bilayers [19]. Furthermore, the range over which the lipid composition can be varied without changing, for example, the phase transition, is larger in monolayers than in bilayers. In the former case, the lipid lateral-packing density and composition can also be controlled independently [131]. Moreover, the intramolecular and the monolayer-subphase in-

teractions can be varied widely by changing the molecule structure (headgroups and hydrophobic chains), the pH or the subphase ion content. Also, and as mentioned above, the internal pressure in biological membranes and phospholipid bilayers cannot be determined directly, because the resultant pressure or tension is zero. In the case of lipid monolayers, the lateral compressibility can be easily accessible from the isotherm slope, providing precise indicators of changes in the film structure [132,133].

## 2.7 Phospholipid monolayers at the liquid/liquid interfaces

In 1964, Brooks and Pethica were the first to design and use a Langmuir trough to compress monolayers at the liquid/liquid interfaces [134]. Using this trough, Pethica and co-workers [135] measured the surface pressure isotherms for a series of insoluble distearoyl-PC (DSPC) and DOPC at the n-heptane/water interface. They concluded that the aqueous electrolyte concentration and pH affected the DSPC monolayers formation, which was found to be independent of the acyl chain length [136]. This conclusion was supported by the absence of any phase transition between 5 and 25 °C observed previously for air/water interface [137], which was in contrast with that observed for PCs having more than 16 carbon atoms [138]. Later, by employing fluorescence and X-ray diffraction techniques, more detailed information on the structure changes and organisation of dipalmitoyl-PC/PE (DPPC/DPPE) monolayers was given [139,140]. Several other studies [58,141–145] of lipid monolayers have mainly concentrated on their characterisation using different kinds of techniques, such as ellipsometry, fluorescence microscopy, and Brewster angle microscopy.

There are relatively few electrochemical studies on lipid monolayers at the air/liquid interface. These studies highlight the investigation of transfer and proton diffusion across different lipid monolayers [146–148]. However, a lipid monolayer at the air/liquid interface is a relatively poor model for a biological membrane, and the ion transfer across it is more conveniently studied at liquid/liquid interfaces using electrochemical rather than Langmuir techniques. For that purpose, an organic solvent is used, allowing sufficient dissociation of organic salts into free ions, and

sufficiently non-polar to avoid significant partitioning of aqueous electrolytes. The monolayers are usually adsorbed on the interface of the bulk organic phase.

In addition to the air/water and solid (mercury)/water interfaces, liquid/liquid interfaces and more specifically the use of the ITIES have been extensively studied as a simplified model for biological membranes. Typically, a liquid/liquid interface consists of two immiscible liquids, usually an aqueous and an organic solution. The advantages of these interfaces are its non-reactive nature, dynamic structure, smoothness, and the possibility to follow ion transfer. The variation of the electrical potential between the two liquids is closely related to the distribution of the ionic and dipolar components across the liquid/liquid interface. In general, there is an excess electrical charge on one side of the interface, which due to the electroneutrality condition has to be compensated by an excess of opposite charge on the other side. Such a charge separation is usually referred to as the formation of the electrical double-layer (discussed in more detail in section 2.9).

Using electrochemical techniques, the characterisation of the interfacial processes and information on the physicochemical properties of the lipid monolayer adsorbed at the ITIES can be obtained, such as the effect of the monolayer state, on the potential distribution across the monolayer, and on ion and electron transfer across it. The advantage of using a single interface formed at the ITIES is that accurate control of the potential drop across the adsorbed monolayer is easily achieved [149], thus allowing the determination of its effect on ion transfer [149, 149–153] and electron transfer kinetics [154, 155].

The first studies of phospholipid adsorption at electrified liquid/liquid interface were presented by Watanabe et al. [156, 157]. These authors measured electrocapillary curves for the electrified interface formed between methylisobutylketone and water and were able to describe and characterise the adsorption of phospholipids. However, the fact that in this study, none or very small amounts of supporting electrolyte was added to the organic phase made interpretation of the results intractable. Later, Girault and Schiffrin [158] studied the adsorption of PCs and PEs from egg yolk at the electrified 1,2–dichloroethane (DCE)/water interface. The electrocapil-

larity data showed a strong dependency of interfacial tension on interfacial potential. Kakiuchi and co-workers studied the adsorption of PCs [149, 159], PE [160], and PS [161] at the nitrobenzene/water interface measuring interfacial capacitance and interfacial tension [162]. These authors and Wandlowski et al. [163] extracted similar Gibbs energies of adsorption for the phospholipids at the liquid/liquid interface, but the former authors suggested weak attractive interactions between the adsorbed molecules, while the latter have suggested weak repulsive interactions. The interaction between aqueous cations and adsorbed phospholipids at the ITIES has also received particular attention, showing that cation complexation can be evaluated and can be responsible for the behaviour observed at more positive potentials [163,164].

Most of the work on lipid monolayers at the ITIES described above focused on the adsorption of lipid monolayers from the bulk organic phase and on the ion permeability of the monolayer [149, 156–162]. A relatively long stabilisation time was needed to reach adsorption equilibrium, and thus a very low reproducibility for the results obtained. Furthermore, the presence of an organic solvent within the monolayer, whose molecules screen the attractive interactions between the phospholipid hydrocarbon tails, led to a more expanded layer [135,136,138,139], thus making the phospholipid environment at the ITIES different from that observed for naturally occurring bilayer structures. Although those systems are easy to use, the amount of adsorbed lipid is limited and the exact state of the layer is uncertain due to the inability to control the monolayer surface pressure [149–152, 159, 161, 165–167].

Several studies can also be found in the literature concerning ion transfer across monolayer-covered liquid/liquid interfaces, initially concentrated on natural mixtures of phospholipids at the ITIES. It is not easy to reconcile the large ensemble of data obtained from the ion transfer studies [152, 160, 163, 168] across lipid monolayers since most of them were obtained on different types of monolayers. Some results have shown that the adsorbed lipid layer has a blocking effect on ion transfer [169], while others pointed to a retardation effect due to the size of the transferring ion and the state of the monolayer [150, 151]. Later studies have also indicated that rather than retardation [170, 171], there is enhancement [172, 173] of

ion transfer across phospholipid monolayers at the ITIES. In fact, the apparent rate constant has been observed to increase in the presence of adsorbed phospholipids for certain cations [149, 152]. Double-layer effects arising from the orientation of the zwitterionic headgroups of PC molecules was the reason given for the observed enhancement [149, 174]. Moreover, specific interactions between transferring ions and the monolayer have also been reported [175]. Recently, the modern electrochemical technique, scanning electrochemical microscopy (SECM), has been used for probing the dynamics and partitioning of electroactive solutes between two immiscible phases [169, 176]. It has been shown with this technique that a DSPC monolayer forms a barrier to the transport of $O_2$, while for DPPC or dimyristoyl-PC monolayers, the transport was not affected at room temperature. By combining SECM–Langmuir techniques, the oxygen transfer kinetics across a DSPC monolayer at air/water and oil/water interfaces were also accessed [148]. It was concluded that the oxygen transfer was very dependent on the state of the monolayer for a given surface pressure, being diffusion-controlled when the monolayer was in the LE phase, and decreasing in the LC state.

## 2.8 Combination of Langmuir–Blodgett and electrochemical techniques at the ITIES

Since it was known that the lipid layer had a great effect on the rate of charge transfer, Grandell and Murtomäki [153, 171, 175], developed a method for simultaneous control of both the surface pressure and the potential drop across of a monolayer at the oil/water interface, by combining the Langmuir technique with the electrochemical control over the interface. Measuring adsorption isotherms of DPPC and DSPC at the air/water and 1,2–DCE/water interfaces, they reported that the latter isotherms did not show a well-defined plateau regions or phase transitions, probably due to the small size of 1,2–DCE molecules, which made them very mobile in the surface phase. At positive potentials, the adsorption of those lipids at 1,2–DCE was weak compared to that at negative potentials where rather stable monolayers were

obtained. However, the transfer of two probe ions, propranolol and picrate, did not show a significant effect of the lipid monolayer on the rate, even at high surface pressures [171].

Unfortunately, this electrochemical Langmuir trough method has some disadvantages: (i) the use of a large interfacial area hampers the electrochemical measurements; (ii) the use of large amounts of toxic organic solvent; (iii) difficulties with monolayer dissolution to the bulk organic phase; and (iv) uneven potential distribution. Electrochemically, this invalidates the use of alternating current (ac) voltammetry or impedance spectroscopy, which are required for quantitative information on the interfacial capacitance and membrane activity of various probe ions.

More recently, to avoid the aforementioned problems, the introduction of a gelled organic phase improved the quality and reproducibility of data, and the monolayer stability as well as the control of lipid packing of monolayers at liquid/liquid interfaces [177–181]. Initially, Kontturi's group developed a new approach to study phospholipid monolayers at the ITIES by combining the LB technique with an immobilised liquid/liquid interface [177]. For that purpose, the lipid monolayer spread at the air/water interface was compressed to a desired surface pressure, and then transferred to an electrochemical cell (containing *o*-nitrophenyloctylether (*o*-NPOE) gelled organic phase) by dipping the cell through the film into the aqueous phase (see Figure 2.7). Since the lipid was transferred on top of the gel, a lipid coated liquid/liquid interface was formed. Interestingly, the solid substrate composed by a gelled organic solvent served simultaneously as a polymer support for the lipid monolayer and an electrochemical half-cell. This study was considered unique in the choice of the substrate. As shown in Figure 2.7, the organic phase was immobilised by a gelling agent, poly(vinyl chloride) (PVC), and the cell made of hydrophobic polytetrafluoroethene (Teflon). Cyclic voltammetry measurements have shown neither inhibition nor enhancement of ion transfer (tetraethylammonium cation, $TEA^+$) kinetics in the presence of a condensed phase DSPC monolayer [177]. It was also shown that the behaviour of the monolayer was dependent of the deposition surface pressure.

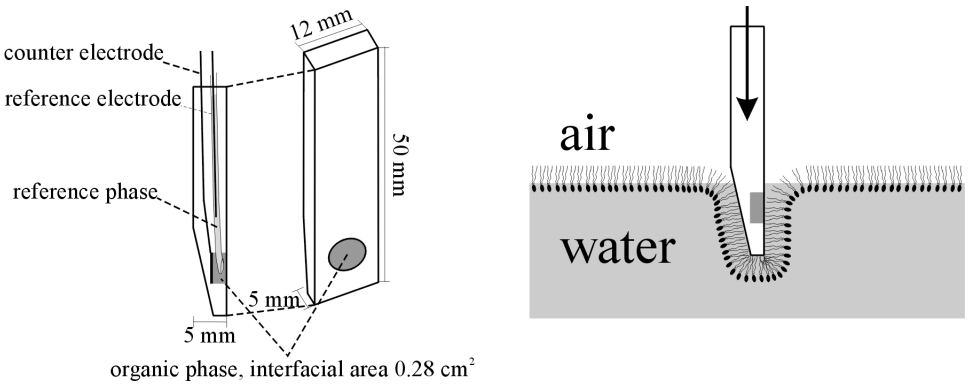


**Figure 2.7.** Schematic representation of the electrochemical half-cell used in electrochemical measurements (left), and LB deposition procedure for producing monolayers at a liquid/liquid interface (right). Reprinted with permission from ref [177]. Copyright © (2000) American Chemical Society.

Subsequently, the described LB-deposition technique was used to probe the membrane activity of ionisable drug molecules both at pure and mixed phospholipid monolayer modified interfaces. The monolayer was characterised with cyclic voltammetry and ac impedance/voltammetry measurements [178–181]. Using these electrochemical techniques, a trend of decreasing ion transfer rate as the surface pressure increases was shown [178, 179], independently of the monolayer composition [178]. With the help of a theoretical model, a mechanism of charge transfer involving an adsorption step was suggested [179].

Furthermore, it has been demonstrated that electrochemistry can be applied to obtain information on drug partition and permeability [180, 182, 183], providing details on charge delocalisation effects, site and strength of drug/membrane interactions of biopharmaceutical interest [180].

## 2.9 Double-layer at the liquid/liquid interfaces

### 2.9.1 Ion transfer at the ITIES

An ITIES can be classified as polarisable or non-polarisable depending on whether a defined relationship exists between the Galvani potential difference between aqueous

and organic phase ($\Delta_o^w\phi = \phi_w - \phi_o$), and the concentrations of ions or electrolytes present. There are two ways to control the potential across the ITIES: (i) by dissolving a single common ion in both aqueous and organic phases (non-polarisable interface); and (ii) with an external electric circuit, when very hydrophilic and very hydrophobic electrolytes are present in aqueous and organic phases, respectively (polarisable interface). The distribution of ions between the two phases is described by the following equation:

$$\Delta_o^w\phi = \Delta_o^w\phi_i^0 + \frac{RT}{z_iF}ln(a_i^o/a_i^w) \tag{2.4}$$

where $\Delta_o^w\phi_i^0$, $z_i$, $a_i^o$ and $a_i^w$ are the standard transfer potential of the ion $i$, the ion charge, and the activities of a common ion $i$ in both phases, respectively. $\Delta_o^w\phi_i^0$, which describes the energy required for transferring an ion from one phase to another, is further given by:

$$\Delta_o^w\phi_i^0 = (\Delta G_{i,tr.}^{w\longrightarrow o})/z_iF = (\mu_i^{0,o} - \mu_i^{0,w})/z_iF \tag{2.5}$$

where $\Delta G_{i,tr.}^{w\longrightarrow o}$ is the Gibbs free energy of transfer of species $i$, $\mu_i^{0,o}$ and $\mu_i^{0,w}$ are the standard chemical potentials of ion $i$ in the organic and aqueous phases, respectively, and $F$ is the Faraday constant. The interfacial potential difference ($\Delta_o^w\phi$) is essentially determined by the salt distribution in both phases. This potential difference is called the *distribution potential*. At a polarisable interface, within a certain applied potential range, no experimentally observable faradaic current flows through the interface before the noticeable transfer of the supporting electrolyte ions. This potential region is known as the *potential window*.

Cyclic voltammetry has been widely used to elucidate reaction mechanisms and to study ion transfer from one phase to another. Basically, this technique involves varying the applied electrode potential as a function of time measuring the resulting current [184]. By varying the potential scan rate, information of the reaction kinetics

and/or the mass transfer process can be obtained. This technique is quite a convenient qualitative method for determining whether a simple electrochemical reaction is limited by diffusion (so-call reversible systems) or completely limited (irreversible systems) or partially limited by kinetics (quasi-reversible systems) [184].

When the surface concentrations are controlled both by kinetics and diffusion, Nernst's law can no longer be used as a boundary condition in the description of the diffusion problem. Under these conditions, the Bulter–Volmer formalism can be applied in the absence of a double-layer effect and may be expressed as follows [184]:

$$k_f = k^0 exp\left(\alpha \frac{z_i F}{RT}(\Delta_o^w \phi - \Delta_o^w \phi_i^{0'})\right) \tag{2.6}$$

$$k_b = k^0 exp\left(-(1-\alpha)\frac{z_i F}{RT}(\Delta_o^w \phi - \Delta_o^w \phi_i^{0'})\right) \tag{2.7}$$

where $\Delta_o^w \phi_i^{0'}$ is the formal transfer potential for ion transfer, $k^0$ is the standard rate constant, and $\alpha$ is the apparent charge transfer coefficient given by:

$$\alpha = (RT/z_i F)(\partial ln k_f / \partial \Delta_o^w \phi) \tag{2.8}$$

This formalism can then be extended to study the adsorption of electroactive species at a liquid/liquid interface [179, 185]. However, it should be stressed that this simple derivation only represents a macroscopic theory, in which the reaction rate is expressed in terms of $\alpha$ and $k^0$. This approach cannot predict how the kinetics is affected by microscopic parameters such as the distance separating the redox species, the nature and structure of the redox species and solvent [184]. The Bulter–Volmer formalism also works well at small overpotentials, but fails to describe the rate at high driving force [184].

The effective $k^0$ for quasi-reversible reactions can be determined from the cyclic voltammograms (CVs), and in particular from the peak potential separation for ion transfer, by applying the following equation [186]:

$$\psi = k^0(D_w/D_o)^{\alpha/2}/[D_w\pi\nu(z_iF/RT)]^{1/2} \quad (2.9)$$

where $D_w$ and $D_o$ are the diffusion coefficients of the transferring ion in water and oil phases, respectively, and $\nu$ is the scan rate. The kinetic parameter $\psi$, is related to the peak separation according to tabulated values for peak separation potentials $\geq 61$ mV [186].

### 2.9.2 Modified Verwey–Niessen model

The electrical double-layer at the oil/water interface is a heterogeneous region that separates two bulk phases of polarised media and maintains a spatial separation of charges. The electrical double-layer at the ITIES was first described by Verwey and Niessen [187] as two non-interacting diffuse layers, one at each side of the interface. Both solvents were assumed to be structureless media with macroscopic dielectric permittivities, and the potential distribution in the electrical double-layer was defined by Gouy–Chapman (GC) theory [188, 189]. The Verwey–Niessen model was later extended by Gavach et al. [190] by introducing an inner layer of oriented solvent molecules in between the two diffuse layers at the ITIES, which is known as the modified Verwey-Niessen model (MVN). This inner layer can either be free of ions or accommodate ions. Although the MVN model has been widely used, the nature of the inner layer has been controversial.

It has been shown that the thickness of the inner layer depends on ionic size and polarity of the organic solvent [191]. It was also observed that the thickness was less than that of a solvent monolayer [191]. This was interpreted to be due to the mixed solvation of ions and interfacial mixing, i.e. the interface consisted of a mixed solvent layer with its composition changing continuously from one media to the other, rather than an ion free layer of either water or organic solvent. Based on interfacial tension and capacitance data, Samec and co-workers [192] suggested that the potential drop across the inner layer was very small while the inner layer capacitance was very high, which would indicate the existence of an orientated

interfacial dipole contribution. It was further suggested that ions could penetrate the inner layer over some distances. To explain these results, the authors have employed the modified Poisson–Boltzmann (PB) theory to all three regions of the MVN model to correct the GC theory by accounting for the finite size of the ions and for image effects. This model is further discussed below in the particular case when phospholipids are added to the organic phase.

### 2.9.3 Theoretical model to interpret adsorbed lipids at oil/liquid interfaces

A majority of the previously cited works in sections 2.7 and 2.8 have used capacitance data to interpret the observed phenomena. In order to get further qualitative information from the experimental results, theoretical models have been developed. In this section, a brief description of some of the models used is given.

It is well-known that a phospholipid monolayer adsorbed at the ITIES induces changes in the electrical structure of the interface. The effect of the monolayer on the rate of ion transfer can be described in a simple way, assuming a sharp interface. A simple electrostatic model (Figure 2.8) based on the solution of the PB equation, where the interface is divided into three layers has been proposed [174, 177] and considers: (i) the organic phase ($x < -d$), (ii) the hydrocarbon region ($-d < x < 0$), and (iii) the aqueous phase ($x > 0$). The phospholipid headgroups are considered to be parallel to the interface and are located at the plane $x = 0$.

The effect of zwitterionic phospholipids on cation transfer across the ITIES from the aqueous to the organic phase, has been described by means of the aforementioned theoretical model [174]. The potential profile in the absence and presence of phospholipids can then be obtained using the GC approach for the aqueous and organic diffuse layers. In this model, the adsorption of aqueous phase cations onto the phospholipid headgroups and the effect of the organic phase cations on the hydrocarbon region via their partition coefficients are taken into account, and no form of the dipole potential is considered. This oversimplification is due to uncertainties concerning the structural contributions of the lipid and water molecules as well as the effect of the applied surface potential and external potential differences on these

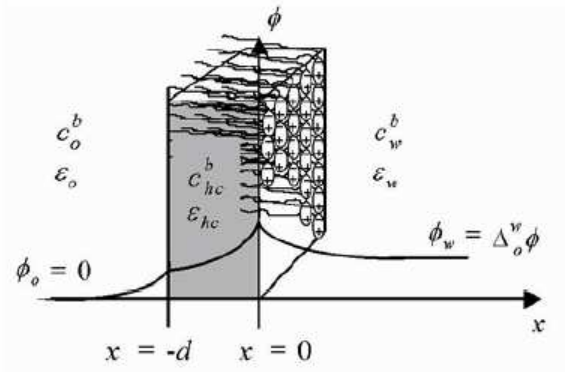


**Figure 2.8.** Drawing of a three-layer model used to describe the potential distribution across the interfacial region. Reprinted with permission from ref [177]. Copyright © (2000) American Chemical Society.

contributions [177].

As shown in Figure 2.8, the hydrocarbon region, the aqueous and organic bulk phases can be represented by their concentrations and relative permittivities, $c_i^b$ and $\epsilon_i^b$, respectively (where $i$ = hc, w, o). As a result of the different permittivities of the organic phase and hydrocarbon region, a chemical partition coefficient, $K_{hc}$, needs to be included when describing the spatial distribution of the organic base electrolyte, and thus $c_{hc}^b = K_{hc}c_o^b$. The surface charge due to the bound cations is given by $\sigma = \alpha e/mmA$ ($e$ is the elementary charge and $mmA$ is the phospholipid mean molecular area in the monolayer). Considering a 1:1 electrolyte case, the electric potential distribution in the region $i$ is described by the PB equation [174, 177]:

$$f\frac{d^2\phi}{dx^2} = \kappa_i^2 sinh[f(\phi(x) - \phi_i)] \tag{2.10}$$

where $\kappa_i = (2F^2c_i/\epsilon_i RT)^{1/2}$ is the reciprocal Debye length in the organic and aqueous electrolyte solutions ($c_i$, and $\epsilon_i$ are the supporting electrolyte concentrations and the solvent dielectric permittivities, respectively), and $f = F/RT$. The following assumptions are considered [177]:

$$\phi_o = \phi_{hc} = \phi(x \longrightarrow -\infty) = 0 \tag{2.11}$$

$$\phi_w = \phi(x \longrightarrow +\infty) = \Delta_o^w \phi \tag{2.12}$$

$$\left(\frac{d\phi}{dx}\right)_{x\longrightarrow\pm\infty} = 0 \tag{2.13}$$

From the integration of equation 2.10 at the boundaries between the different regions, the electric potential gradient is obtained from [174, 177]:

$$f\left(\frac{d\phi}{dx}\right)_{x=0^+} = 2\kappa_w sinh\left(\frac{f(\Delta_o^w\phi - \phi(0))}{2}\right) \tag{2.14}$$

$$f\left(\frac{d\phi}{dx}\right)_{x=-d^-} = 2\kappa_o sinh\left(\frac{f\phi(-d)}{2}\right) \tag{2.15}$$

$$f^2\left(\frac{d\phi}{dx}\right)^2_{x=-d^+} - f^2\left(\frac{d\phi}{dx}\right)^2_{x=0^-} = 2\kappa_{hc}^2(cosh[f\phi(-d)] - cosh[f\phi(0)]) \tag{2.16}$$

The solution of equation 2.10 is obtained by relating the two GC electrical potential profiles by employing the continuity of the dielectric displacement [174, 177]:

$$\epsilon_o\left(\frac{d\phi}{dx}\right)_{x=-d^-} - \epsilon_{hc}\left(\frac{d\phi}{dx}\right)_{x=-d^+} = -\sigma \tag{2.17}$$

$$\epsilon_w\left(\frac{d\phi}{dx}\right)_{x=0^+} - \epsilon_{hc}\left(\frac{d\phi}{dx}\right)_{x=0^-} = \sigma \tag{2.18}$$

where $\sigma$ is the surface charge. The ion size is neglected or it is considered that the plane of adsorption coincides with the plane of the phospholipid headgroups. The potentials $\phi(0)$ and $\phi(-d)$ are obtained by solving the system of equations ( 2.14, 2.15, 2.16, 2.17, and 2.18) [177]:

$$(c_o^b\epsilon_o - c_{hc}^b\epsilon_{hc})cosh[f\phi(-d)] = (c_o^b\epsilon_o - c_{hc}^b\epsilon_{hc}cosh[f\phi(0)]) +$$

$$\left((2c_w^b\epsilon_w)^{1/2}sinh\left[\frac{f\left(\Delta_o^w\phi - \phi(0)\right)}{2}\right] + \frac{\sigma}{(4RT)^{1/2}}\right)^2 \tag{2.19}$$

Since the whole system is electroneutral, $Q_i + \sigma = 0$, where $Q_i$ is the charge in the phase $i$. The interfacial capacitance is defined as:

$$C = \frac{\partial Q}{\partial \Delta_o^w \phi} \tag{2.20}$$

where $Q$ is the surface charged density separated across the ITIES, and can be evaluated as [177]:

$$Q = -Q_o - Q_{hc} = Q_w + \sigma = \int_0^\infty \rho dx + \sigma = 8RTc_w^b\epsilon_w sinh\left[\frac{f(\Delta_o^w\phi - \phi(0))}{2}\right] + \sigma \tag{2.21}$$

The interfacial capacitance is calculated by numerical differentiation using equation 2.20. In equation 2.21, $\sigma$ is also a function of the total potential drop, and the interfacial potential $\phi(0)$ is also naturally potential dependent. Using the theoretical model presented above, Liljeroth et al. [177] suggested that the negative shift observed in the minimum of the capacitance curves was due to the aqueous cation binding to the zwitterionic phospholipid (DSPC), and that the lowered values of the interfacial capacitance was due to the decrease of the dielectric constant and to the decrease of the organic electrolyte concentration in the monolayer hydrocarbon domain. This model can then be modified and extended for 2:1 electrolytes, which is further discussed in chapter 4.

### 2.9.4 Ac impedance/voltammetry

The interfacial capacitance can be measured with ac impedance/voltammetry. Although cyclic voltammetry can be used to study kinetics of an electrode reaction,

the result is often corrupted by side-effects, such as charging double-layer currents or by ohmic drop associated with the experimental setup [184].

Ac impedance/voltammetry has been widely used to study electrical double-layer effects, electrode kinetics, corrosion, etc., and has also been used in most of the studies mentioned in section 2.7 and 2.8. The ac response considers an electrochemical system as linear, i.e. that the current response for small potential perturbations is linear, and the potential for small imposed current perturbations is also linear (for amplitudes $< 20$ mV) [184]. The impedance is given by [184]:

$$Z = dE/dI \tag{2.22}$$

or in its complex form:

$$Z = Z' - iZ'' \tag{2.23}$$

where $Z' = |Z|\cos(\phi)$ and $Z'' = |Z|\sin(\phi)$ are the real and the imaginary impedances, respectively, and $\phi = \arctan(Z''/Z')$. The impedance magnitude can be calculated as:

$$|Z| = [(Z')^2 + (Z'')^2]^{1/2} \tag{2.24}$$

Assuming that the interfacial system can be treated as an equivalent circuit, often referred to as the Randles circuit, and provided that the solution resistance is completely compensated for, the interfacial double-layer capacitance can be obtained from [184]:

$$Y = Y_{C_{dl}} + Y_W = j\omega C_{dl} + [R_{ct} + \sigma'(\omega)^{-1/2}(1 - j)]^{-1} \tag{2.25}$$

where $Y$ is the total admittance of the elements in parallel, $C_{dl}$ is the double-layer capacitance, $W$ is the Warburg impedance, $R_{ct}$ is the charge transfer resistance, $\omega$

is the angular frequency of the applied ac potential, and $\sigma$' is the Warburg diffusion coefficient. The impedance is given by the inverse of equation 2.25.

Ac impedance is then measured as a function of the frequency of the ac source, and the output is a plot of the cell or electrode impedance plotted vs frequency. Similar results can be obtained by employing ac voltammetry. Ac voltammetry is basically a faradaic impedance technique, and consists of adding a small amplitude sinusoidal potential onto a linear potential ramp, and measuring the ac current. Briefly, a potential $E_{dc}$ is imposed potentiostatically at arbitrary values that usually differ from the equilibrium value. Usually, $E_{dc}$ is varied systematically on a long time scale compared to that of the superimposed ac variation (10–100 Hz). The output is a plot of the magnitude of the ac component of the current versus $E_{dc}$.

## 2.10 Brief introduction to colloid metallic nanoparticles: synthesis and applications

Gold (Au) nanoparticles (NPs) or colloid Au have been known and used since ancient times, for example, to colour glass. However, only in 1857, Faraday prepared the first pure sample of colloidal Au which he called "activated gold" [193]. He was the first to recognise that the colour was due to the minute size of the Au particles, using the term "divided metals" to describe the deep-red Au sols resulting from the reduction of a Au chloride solution with phosphorus. Nowadays, these nanoscale materials are defined as a dispersion (or colloid) of a solid phase of sub-micrometer-sized particles in a liquid phase (aqueous or organic) with physical dimensions varying from 1 to 100 nm.

Advances in NP research have prompted the development of techniques that have subnanometer resolution. As a consequence, an exponentially increasing number of publications concern the potential use of the NPs in nanoscience and nanothecnology, due to their chemical, optical, electronic, and magnetic properties. NP properties differ from those of bulk materials and isolated atoms or molecules, and are dependent on the particle size, shape, and surface modification. Recently, bio-

logical applications have focused on the targeted drug delivery, with tailoring of the functional properties of the particles. When combined with polyelectrolytes, these polymeric particulate systems can target specific tissues.

The following sections focus mainly on the description of Au and ruthenium (Ru) NPs, their preparation and applications, focusing on the important aspects that are relevant to the present work.

### 2.10.1 Preparation of nanoparticles

The supermolecular organisation of NPs is an important prerequisite for applications in the field of nano(bio)technology. The development of synthesis protocols for nanostructured materials with tunable physicochemical properties is therefore an important goal. In the past years, NPs, and in particular AuNPs, have received considerable attention, showing interesting applications in single electron tunnelling [194], non-linear optical devices [195], and in DNA sequencing [196], among others. They are commercially available in many forms, and several methods to synthesise AuNPs over a range of sizes [197, 198], and shapes [199], have been described in the literature. The use of AuNPs is often limited, however, by their polydispersity.

Several methods have been developed to prepare AuNPs. Most reports on the synthesis of AuNPs in non-polar organic solvents have followed the Brust–Schiffrin method [200, 201]. Briefly, aqueous chloroaurate ions ($AuCl_4^-$) are transferred into the organic solvent (toluene) using phase transfer molecules (tetraalkylammonium salts, e.g. tetraoctylammonium bromide). $AuCl_4^-$ ions are then reduced upon addition of sodium borohydride ($NaBH_4$) and capped with alkanethiol [200, 201]/alkylamine [202] (e.g. dodecanethiol) molecules resulting in stable AuNPs that can be stored as a powder. NPs can be readily redispersed in a range of non-polar to weakly polar organic solvents for use as novel reagents.

Although simply prepared, most of the NPs synthesis reported in the literature yield NPs that are only soluble in organic solvents. However, a fundamental prerequisite for the use of NPs in biological applications is that they should be easily dispersible in water because they must combine with macromolecules in aqueous solu-

tion [203]. Recently, AuNPs have been synthesised by Chen and Kimura [204] using a one-phase reduction method. Following this method, caboxylate-modified AuNPs have been synthesised based on the reduction of $AuCl_4^-$ by $NaBH_4$ in methanol using mercaptosuccinic acid (MSA) as the stabilising ligand. As a result, negatively charged water-soluble MSA-AuNPs and with a size distribution between 1–3 nm were obtained. These AuNPs can be precipitated and redispersed in water without further aggregation, which represents an advantage compared with other aqueous gold colloids that suffer from easy aggregation [200, 205–208], and cannot be used as concentrated solutions [203]. Moreover, carboxylate-modified sized particles as small as 1 nm, are excellent candidates, for example, in cell-biology electron microscopy studies.

Recently, the synthesis of dextran/AuNP hybrid material for biomolecule immobilisation and detection has been described [209]. The idea was to use the versatility of dextran for attachment of biomolecules and combine it with the optical properties of metallic NPs in order to provide a platform where ligands can be introduced and their specific interaction with the corresponding proteins can be studied with optical techniques. The interaction of macromolecules of biological interest with lipid membranes is also important in various areas like membrane biophysics and drug formulations [210, 211].

Other charged particles of great interest are Ru NPs. Ru is an important member of Pt group metals, and it is widely used for the selective hydrogenation of carbonyl groups in the vicinity of conjugated or nonconjugated C=C double bonds hydroxyl groups as well as in partial hydrogenation of aromatic compounds. Ru metal NPs, in particular, are well-known for their catalytic activity. They have been prepared with stabilisers such as polymers [212] and ligands [213–215], with different shapes and particular control of the particle size. Again, most of these preparations are carried out in organic solvents and the NPs prepared are not water-dispersible. To self-assembly Ru NPs (or others) with biomolecules templates, positively charged Ru NPs were recently easily prepared in aqueous medium [215] using $NaBH_4$ as the reducing agent and by setting the pH value of the reaction medium below 4.9.

This method allowed the formation of Ru NPs with an average diameter of 1.8 nm, providing new opportunities for surface functionalisations of biological ligands such as polyelectrolytes, DNA, and oligonucleotides that may be attached to the Ru surface.

### 2.10.2 Polyelectrolyte/nanoparticle multilayer films

The layer-by-layer (LbL) self-assembly of polyelectrolytes represents a general and powerful method to build tailored ultrathin films of well-defined thickness, composition and structure. Decher and co-workers [216] were the first to develop this simple approach that yields nano-architecture films with good positioning of individual layers, but rather independent of the nature, size and topology of the substrate [216]. The multilayer structures composed of polyion or other charged molecular or colloidal objects are fabricated by strong electrostatic attraction between an oppositely charged surface and molecules in solution. Since the process involves only adsorption from solution, there are in principle no restrictions with respect to substrate size and topology. The advantage of this technique is that film deposition on glass slides can be carried out manually or by an automated device. Other advantages of LbL adsorption from solution are that several different materials can be incorporated in individual multilayer films and that the film architecture is determined only by the deposition sequence. This simple idea of LbL assembly by adsorption from solution has opened an avenue for the fabrication of multicomponent films on solid supports.

Polyelectrolytes, such as GAGs, are substances in which the monomeric units of their constituent macromolecules have ionisable groups. The most important property of polyelectrolytes is their water solubility giving rise to a wide range of nontoxic, environmentally friendly, and cheap formulations. A polyelectrolyte is always composed of a macroion where the charged groups are interconnected by chemical bounds, together with an equivalent number of small oppositely charged counterions. This association leads to loose bound counterion clouds around the polyelectrolyte chains. This section will not focus on the polyelectrolytes themselves, but on the possible interactions between them and nanostructured materials, such

as NPs (and in particular AuNPs).

There is at the present considerable interest in the use of nano-objects for various applications involving mainly the physicochemical properties of NPs, that depend on several factors, such as: (i) the particle size and size dispersity; (ii) the structure of the particles; (iii) the surface and shape of the particles; and (iv) the organisation of the particles into a nanomaterial and their dispensability. All these factors are also dependent on the successful control, including reproducibility, of the synthetic process and the stability of the particles.

A large number of advanced techniques have been applied to the characterisation of nanomaterials, such as TEM, X-ray scattering, X-ray photoelectron spectroscopy, and zeta-potential measurements [216–218], among many others. The LbL has been the most widely employed to study protein [219, 220], polyelectrolyte/polyelectrolyte [216,217,221], polyelectrolyte/surfactant [222,223] and polyelectrolyte/NP [224–231] multilayer assemblies. These kind of assemblies are of great interest due to promising applications in different fields such as membranes [232, 233], drug delivery [221, 234, 235], chemical and biological sensing [218, 236], nanotechnology, semiconductors, molecular electronics, photovoltaic cells, and catalysis [218, 236, 237].

Research on polyelectrolyte/NP multilayers has increased significantly, especially in the context of nanoscience and nanotechnology. AuNPs or Au colloids have been extensively used to build-up multilayers, mainly because they are the most stable metal NPs, and because of their size-dependent behaviour as individual particles, and their electronic, magnetic and optical properties [238]. It has been demonstrated that stable polyelectrolyte/AuNP multilayers can be used to fabricate nanocomposites of differently modified NPs and polyelectrolytes as well as to construct covalently attached organic/inorganic multilayer hybrids [224]. The growth of polyelectrolyte/NP films containing monolayer-protected Au clusters takes place through the assembly of multiple monolayers of NPs, polyelectrolyte chains looping/entangling with charged NPs [226]. Fabrication of self-assembled polyelectrolyte/AuNP multilayer films has shown that the film can behave as a wide-band-

gap semiconductor, with a very reduced multilayer thickness [227].

Electrochemistry is a powerful tool to study these systems. Polyelectrolyte multilayers formed at the NPOE/water interfaces is a new approach in the study of drug release [221]. Cyclic voltammetric data of LbL self-assemblies of oppositely charged polyelectrolytes anchored to a lipid monolayer has shown no decrease of the transfer rate of $TEA^+$ until the deposition of the seventh negatively charged polyelectrolyte layer. On the other hand, with the same system, $TEA^+$ transfer was already retarded after the deposition of the fourth positively charged layer. Moreover, comparison of $TEA^+$ and tacrine transfer across the polyelectrolyte indicated an effect of the shape and charge delocalisation of the transferring ion on the apparent rate constant. It has also been demonstrated that facile electron and ion transfer occurs through multilayers of Au nanoclusters covered by self-assembled monolayers of alkylthiols with various functional groups [239]. With this system, electron transfer between a ferrocene moiety and the Au electrode has been described to occur through the Au nanocluster cores by a hopping mechanism. Using SECM, Ruiz et al. [229] measured the lateral and cross-film electron transport in the polyelectrolyte/AuNP multilayers attached electrostatically to an inert substrate. The conductivity of a single AuNP monolayer was quantified, demonstrating that subsequent layers are not electrically insulated from each other and that there is significant communication between NPs in different layers. More recently, the charge transport through poly(L-lysine) (PLYS)/MSA-AuNPs attached electrostatically to Au surfaces have been reported [240]. Using AFM, STM, electrochemical techniques, and a theoretical model, the authors showed that the transfer mechanism for $[Fe(CN)_6]^{3-/4-}$ species involved a non-linear slow diffusion through defects (pinholes) in the multilayer, whereas electron transfer through the AuNPs was the dominant mechanism in the case of $[Ru(NH_3)_6]^{3+/2+}$. Furthermore, it was shown that the PLYS film contribution to the tunnelling barrier was negligible, and the overall kinetics was controlled by the electron exchange between the ferri/ferrocyanide redox couple and the particles [241].

All these results have shown that AuNPs can greatly improve the conductivity

and the electron transfer ability in the films. Therefore, polyelectrolyte/AuNP films have also been suggested as possible electrochemical sensors due to their electronic and catalytic properties, for example in the detection of NO [242].

Microcapsules can also be fabricated by LbL, where the core is dissolved and the remaining shells serve as capsules for materials such as polymers, enzymes, etc. The great advantage of such materials is that they allow the composition of their walls to be tailored to incorporate metal NPs. For example, biocompatible polyelectrolyte multilayers (such as DS and other polysaccharides) have been used to encapsulate ibuprofen microparticles for the purpose of controlled release [243]. More recently, polyelectrolyte multilayers have also been used to encapsulate Au sulfide core/Au shell NPs, and using laser real-time fluorescence, the release of the NPs was followed [244]. The methods and technology presented, were considered to be of interest for drug delivery.

Despite the large number of polyelectrolyte/NP multilayers studies in the literature, very few of them concern water-soluble NPs. As stated previously, this is a very important aspect for future biological applications [203, 245].

## 2.11 Isothermal titration calorimetry: thermodynamic parameters

ITC can provide a full thermodynamic characterisation of binding events [246], by measuring the heat exchange on the formation of a complex directly. It is a very simple technique which enables the entire set of thermodynamic parameters to be obtained by performing relatively few experiments at different temperatures. In contrast to spectroscopic methods that have been widely applied to investigate, for example, unfolding and refolding pathways of proteins, calorimetric methods are more advantageous due to the fact that they do not require intrinsic chromophores to report on the conformational state of the macromolecules under investigation. Conformational changes in proteins and peptides have successfully been investigated with ITC [247].

The difficulty in measuring heat exchange lies in the fact that this parameter, which is the immediate outcome of ITC, is an integral property of whole system, and therefore, it is not easy to separate all its components. The total heat contains contributions arising from non-specific effects, such has heat of dilution of the titrant into buffer, incomplete match of the temperatures of the solutions in the cell or at the injection syringe tip, and heat effects from mixing of buffers of slightly different chemical composition. The measurement is based on the electric compensation of the heat which is released or taken up by the system during the titration. In an ideal case, no reaction heat will be monitored after the host molecules have been complexed. Binding enthalpy ($\Delta H$), binding constant ($K_b$), and stoichiometry can be determined by integrating the heat of each individual titrant injection, and fitting the obtained enthalpy curve to a chosen binding model. The Gibbs free energy ($\Delta G$), entropy ($\Delta S$), and heat capacity ($\Delta C_p$) are calculated from the fundamental equations:

$$\Delta G = -RTlnK = \Delta H - T\Delta S \tag{2.26}$$

$$\Delta C_p = \frac{\partial(\Delta H)}{\partial T} \tag{2.27}$$

### 2.11.1 Enthalpy, entropy, and heat capacity

In ITC, the $\Delta H$ is measured during the titration, and therefore, is a probe of the amount of ligand bound at each injection. $\Delta H$ is associated with the contribution of formation, or breaking of non-covalent bonds in the system. Information on the change in order of the system, such as changes in conformation as well as effects of the binding or release of solvent molecules are referred to $\Delta S$ [248]. Additionally, the chemical nature of protonation/deprotonation events concurrent with the binding reaction, are also evaluated from $\Delta H$.

Hydration effects of a complex are described by $\Delta S$ as a consequence of the large hydration of polar and apolar groups and significant reduction of the water accessible surface during binding [246]. Consequently, when a complex is formed,

the overall $\Delta S$ is often large and positive. Sometimes ordering of water at the interface of the complex occurs, which contributes unfavourably to $\Delta S$ ($< 0$) and favourably to $\Delta H$ ($< 0$) [249]. Furthermore, unfavourable contribution to $\Delta S$ can also originate from the reduction of the side chain mobility at the binding site [246]. However, negative $\Delta S$ does not necessarily indicate that the hydration of the interface remains unchanged. On the other hand, positive $\Delta S$ has been referred to as a strong indication that water molecules have been expelled from the interface of the complex [246].

It has been observed that heat capacity, $\Delta C_p$, is almost always negative when the complex is taken as the reference state, i.e. the complex has a smaller $\Delta C_p$ than the sum of its free components. Experimental and theoretical observations have indicated that $\Delta C_p$ originates from changes in the degree of surface hydration in the free and the complexed molecules, and also to a lesser extent from changes in molecular vibrations [250].

As a result of calorimetric studies on the transfer of organic compounds to aqueous solvents and on protein folding/unfolding equilibria, a correlation between the burial of the bimolecular surface area and $\Delta C_p$ has been observed [248, 250]. This effect is described by considering the ordering of water molecules on a hydrophobic surface and that their non-covalent bonds having energetically different vibrational modes result in a different $\Delta C_p$ to water in the bulk solvent. Although the burial of hydrophobic surface area gives the largest contribution to $\Delta C_p$, effects of polar surfaces may also affect the observed $\Delta C_p$ [248, 251, 252]. Therefore, $\Delta C_p$ determinations for individual interactions give valuable information on the aromatic and non-aromatic apolar groups contribution as well as on the conformational states and vibrational contents between the complex and its free components.

The incorporation of water molecules at biomolecular interfaces seems also to be very important in drug interactions. The release of the water from the interfaces is generally considered to provide a favourable contribution to $\Delta G$ of binding based on the increase in the overall degrees of freedom of the system on going from free to bound state [248]. Consequently, water molecules are fundamental in drug design

[253] and in stabilising drug/protein interactions [254].

### 2.11.2 Thermodynamic studies using ITC

Efficient interaction with phospholipidic bilayers and the ability to permeate cell membranes are parameters of indubitable importance for the design of pharmacological active molecules. Therefore, it has become of central importance to understand the correlation between structural details and the thermodynamic measurements of an interaction.

ITC studies have concentrated mainly on carbohydrate/drug/protein–protein interactions. Calorimetric studies have shown that the interaction of amphiphilic drugs with a biomembrane model can be improved by using drug/lipoamino acid complexes. These acids modify the physicochemical properties of drugs (lipophilicity and amphiphilicity), which under certain conditions may increase the adsorption of drugs through cell membranes and biological barriers [255]. Furthermore, the binding of a peptidomimetic drug with phosphotyrosine substituted by a benzylmalonate moiety have shown a lower $K_b$ (8.5 x $10^4$ $M^{-1}$) than a tyrosyl phosphopeptide standard ($K_b$ = 2.5 x $10^6$ $M^{-1}$) [256]. This was attributed to a significant reduction in $\Delta S$, due to partial restriction of the degrees of freedom of additional bonds and hydration state changes of the benzylmalonate group.

Among others, ITC has been the most commonly used for quantitative analysis. Thermodynamic parameters of the interaction between proteins and HS/heparin have been extensively studied in the literature [257–259]. Recently, it has been demonstrated that cell-penetrating peptides bind to HS and liposomes vesicles with an association constant of 3.1 x $10^6$ and 3.1 x $10^4$ $M^{-1}$ at 28 °C, respectively. $\Delta H_{pep}$ = –5.5 kcal/mol with about 7 molecules of peptide bind per HS chain was observed [258]. The observed positive $\Delta C_p$ (+167 cal $mol^{-1}$ $K^{-1}$) was attributed to the hydrophobic forces in the binding, or in some cases, due to a charge neutralisation reaction [257]. In a similar study, for the binding of HS with Melittin (an amphiphatic cationic peptide), a negative $\Delta C_p$ (–45 cal $mol^{-1}$ $K^{-1}$) was found [259, 260]. This was understood to be due to both electrostatic and hydrophobic interactions.

Swaminathan and co-workers [261] have shown that some membrane receptor/protein interactions led to exothermic binding between 6.4 and 42 °C, with a large negative $\Delta C_p$ value. Interestingly, they also observed negative $\Delta S$ (an unusual feature among protein/protein interactions), that turned positive below a temperature of 20.4 °C. Furthermore, an unchanged free energy ($\Delta G \approx 0$) of interaction due to enthalpy-entropy compensation was attributed to solvent reorganisation and release of water molecules from the vicinity of the binding site. Similar results have also been reported for the binding of galactose-like carbohydrate to agglutinin protein as well as for drug/globular protein (tubulin) interactions [262], indicating that the reorganisation of water molecules in these systems play an important role in the binding process [263]. In the latter study, drug-induced conformational changes in the protein were observed by the quenching of intrinsic fluorescence, showing that an alteration in the position of a single substituent on the backbone of a drug molecule led to either large positive or negative $\Delta C_p$ values. These results were interpreted considering a combination of hydrophobic and van der Waals interactions as well as hydrogen bonding between specific groups in the drug/tubulin complex.

# 3 Outline of the Present Study

As discussed in chapter 2, despite intensive research knowledge about fundamental physicochemical and biological aspects, the interactions between the different components of the biological membranes as well as the mechanisms through which ions and drugs can cross them are still incomplete and unclear. Therefore, new and more complex model membranes need to be considered. In line with this, the major aims of the present study were:

(*i*) To modify the phospholipid monolayers with DS in the presence of calcium.

(*ii*) To self-assemble polyelectrolyte/AuNP multilayer films on phospholipid monolayer modified with DS.

(*iii*) To prepare and electrochemically characterise DS-modified Ru NPs.

(*iv*) To incorporate gA into phospholipid monolayers in the presence of DS.

(*v*) To determine thermodynamic parameters of binding between GAG and drug molecules.

(*vi*) To investigate the interactions between model lipid membranes and GOx.

# 4 Main Results and Discussion of the Published Work

In this chapter, a summary of the most important results obtained from the publications listed at the beginning of the thesis is presented and discussed. The following subsections refer to different techniques applied to characterise the physicochemical properties of the systems under study.

## 4.1 Interaction between lipid monolayers and DS, polyelectrolyte/AuNP multilayers, and gA at an air/liquid interface (I–IV)

Although the interactions between lipids and DS have been extensively studied in the past, there is still uncertainty about the mechanism. Furthermore, studies involving polysaccharides or proteins and lipid monolayers using electrochemical methods are scarce. As shown in the literature review chapter, a surfactant monolayer spread at the air/liquid interface gives valuable information on molecular interactions, and therefore, this interface was used to obtain further information in the present study.

### 4.1.1 Isotherms of saturated lipid monolayers (I, VI)

Compression isotherms of lipid monolayers spread on an aqueous subphase were first recorded in a Langmuir trough. The subphase contained $Ca^{2+}$ ions in 3 mM concentration to mimic the extracellular fluid. Isotherms were recorded both in the absence and presence of DS. $Ca^{2+}$ ions were used to create an attractive electrostatic interaction between the lipid surfaces and DS. The lipid/DS interactions were accessed from the isotherms shown in Figure 4.1.

In the absence of DS, the isotherms of a zwitterionic (DPPC) and negatively charged (dipalmitoyl-PA (DPPA)) lipid, behaved similarly to those in the literature [106, 147, 264]. In contrast, different behaviour was observed when DS was added to the subphase. In the case of DPPC, the main phase transitions at a surface

pressure of 10 mN/m was not observed after the formation of the DPPC/$Ca^{2+}$/DS complexes, suggesting that DS did not penetrate into the lipid monolayer, but was adsorbed and bound to the lipid headgroups by coulombic interactions via $Ca^{2+}$ ions. The compressibility modulus, $C_s^{-1}$, was slightly lowered in the absence of DS, which can be explained by the closest packing of the lipid molecules as a result of the strong cohesive interactions between the carbon chains. Interestingly, at high surface pressures, the isotherms in the absence and presence of DS almost overlapped with each other, which is understood to be due to breaking of the $Ca^{2+}$ bridges [265]. Consequently, DS desorbed from the surface.

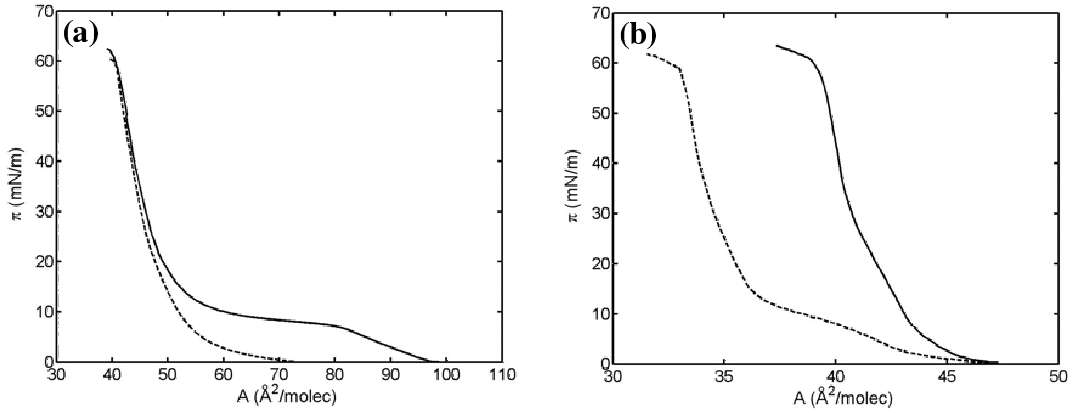


**Figure 4.1.** $\pi$–$A$ isotherms of DPPC (a) and DPPA (b) monolayers spread onto a 3 mM $Ca^{2+}$ aqueous subphase in the absence (solid line) and presence (dotted line) of coupled lipid/$Ca^{2+}$/DS complexes at $T = 20.0 \pm 0.1$ °C. Reprinted with permission from publication I. Copyright © (2005) American Chemical Society.

On the other hand, for a DPPA/$Ca^{2+}$/DS hybrid layer, new phase transitions were observed in the isotherms, in contrast to that observed in the absence of DS. This behaviour has also been described elsewhere for DPPA monolayers in the presence of a positively charged copolymer, poly(diallyldimethylammonium chloride) [106, 264]. The adsorption of DS to DPPA monolayers was stronger than to DPPC monolayers, which can be deduced from the more condensed lipid isotherm as well as from the higher $C_s^{-1}$ in the DPPA case compared with DPPC.

The interactions between the two lipids and DS were further verified by atten-

uated total reflection (ATR)–FTIR. These experiments were performed with DPPC and DPPA multilayers transferred onto a Ge substrate. From the ATR spectra of DPPC, DS characteristic bands were observed, but after DS was added to the lipid monolayer, the band at 1239 $cm^{-1}$, assigned to the asymmetric P=O stretching of the $PO_2^-$ group [266], was much broader than in the absence of DS, due to the asymmetric stretching of the S=O bond [267]. This result showed that DS was an integral part of the transferred monolayer system, and confirmed the LB and electrochemical results. Furthermore, the lipid/DS spectrum showed strong water bands around 1640 $cm^{-1}$, which indicated that water molecules were included in the complex multilayer. All these results supported very well the electrochemical data.

$\pi$–$A$ isotherms were also used to monitor the interfacial interactions between GOx and DPPC (unpublished results). In the absence of lipid, GOx isotherms showed a phase transition plateau at a surface pressure of 8 mN/m, while in the presence of lipid, two clear phase transition points were observed: one at a surface pressure of 5 mN/m and another at 8 mN/m. This result is a clear evidence of GOx incorporation into the DPPC monolayer, which supports the results of publication VI.

### 4.1.2 Isotherms of unsaturated lipid monolayers (II–IV)

In publication II, isotherms of a cationic lipid, dioleoyloxy-propyl-trimethylammomium chloride (DOTAP) were measured. The subphase contained either NaCl + DS or NaCl + AuNPs. Addition of DS led to a more expanded isotherm than that observed for pure DOTAP or for DOTAP + AuNPs, showing also high compressibility. This was explained by the overcompensation of negative charge of AuNPs and DS strands by the positive charge of the lipid headgroup molecules. On the other hand, adjacent AuNPS and DS strands repelled each other, hence expanding the monolayer.

The interaction between unsaturated lipids (palmitoyloleoyl-PC, POPC; PO-phosphoglycerol, POPG) and DS-modified Ru NPs (referred as composite nanoclusters) were also investigated by $\pi$–$A$ isotherms (publication III). The analysis of the

isotherms showed rather rigid monolayer films of either the zwitterionic (POPC) and negatively charged (POPG) lipid. Interestingly, and as observed for DOTAP monolayers, the adsorption of composite nanoclusters to the lipid monolayers led to more expanded isotherms than with pure lipid only, but no significant changes in the phase transitions of the lipids were observed. However, a slightly higher collapse pressure was observed in the presence of composite nanoclusters in the subphase. As in publication I, also here $Ca^{2+}$ ions mediated the binding between the lipids and the composite nanoclusters, leading to the formation of lipid/$Ca^{2+}$/nanocluster complexes.

In publication (IV), the model membrane was improved by incorporating a channel-forming peptide (gA) into the lipid monolayers, in order to study lipid/gA and lipid/gA/$Ca^{2+}$/DS interactions. Gramicidin A was dissolved in chloroform. It is itself a surface active compound and undergoes phase transitions [51, 56, 57, 59] as shown by its isotherms (Figure 4.2a). When DS was added to the subphase, the gA monolayers were slightly expanded, in a similar way as reported in publication III. In order to study the lipid/gA interactions, different mixed lipid/gA monolayers were measured by compression isotherms. The isotherms of mixed monolayers appeared to depend on the lipid/gA molar ratio, but not on the lipid headgroup, since similar results were obtained for POPC/gA or POPG/gA monolayers. Furthermore, the Langmuir technique also showed that the studied systems were not affected significantly when DS was added to the subphase. To get further insight on the properties of the monolayers of this complex system, the $mmA$ of the mixed monolayers was calculated as the sum of the individual $mmA$ of both lipid and gA monolayers at a given surface pressure:

$$mmA = X_L A_L + (1 - X_L) A_{gA} \tag{4.1}$$

In equation 4.1, $X_L$, $A_L$, and $A_{gA}$ are the molar fraction of the lipid, and the experimental $mmA$ of the pure lipid and gA monolayers, respectively. The calculated isotherms (Figures 4.2c and 4.2d) confirmed that the hybrid monolayer was not just due to non-interacting molecules, occupying certain molecular area, but an attractive

lipid/gA interaction existed, which led to a more packed structure [51]. From the analysis of equation 4.1 and compressibility data for all the studied monolayers, it was suggested that there were void spaces between gA molecules, which were occupied by lipids in a mixed layer. As a consequence, the mixed monolayer became more flexible than pure monolayers due to the disruption of the structure. On the other hand, small differences were observed between PC and PG headgroups, which were attributed to hydrogen bonding and hydration properties.

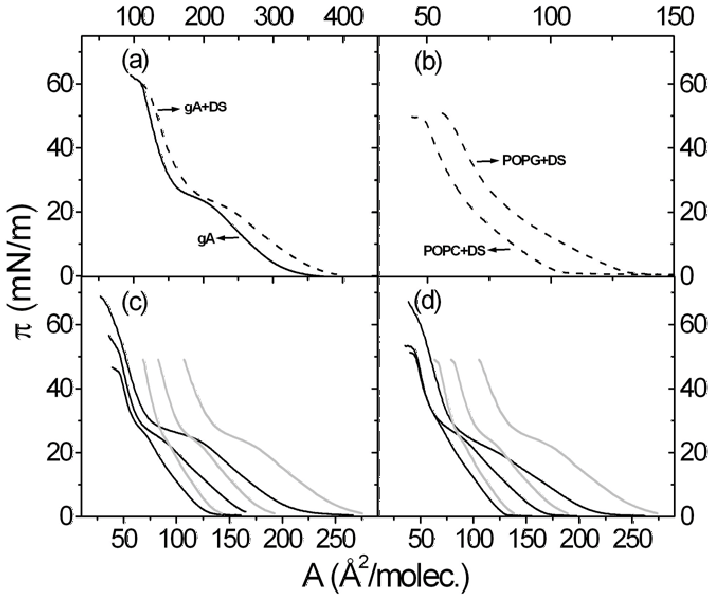


**Figure 4.2.** $\pi$–$A$ isotherms measured at 20.0 ± 0.1 °C for gA (a), POPC and POPG (b); mixed POPG/gA (c) and POPC/gA (d) monolayers at molar fractions of 91, 71, and 38 mol% of lipid (from the left to the right). Theoretical isotherms [solid grey lines (c) and (d)] for the same molar fractions. Reprinted with permission from publication IV. Copyright © (2007) Wiley-VCH Verlag GmbH & Co. KGaA.

## 4.2 Electrochemical characterisation of lipid monolayers modified at a liquid/liquid interface (I–IV, VI)

### 4.2.1 Interfacial capacitance

After characterisation of the monolayers by compression isotherms, the different monolayer systems were transferred to an aqueous/organic gel interface using the LB technique in a controlled manner as described in section 2.8, and the physicochemical properties of a specific system were studied at the ITIES. The interaction between the lipid monolayer and the DS presented in the bulk solution, and their respective impact to the capacitance, was derived from the ac voltammetry. This method can give sensitive information on the potential-dependent properties of the monolayer [178, 180, 181] and has also been successfully employed to study the interactions between polysaccharides and lipid monolayers at a solid/liquid interface [268]. The capacitance data was analysed by using a simplification of the Randles equivalent circuit. Considering that the transfer of the supporting electrolyte ions is diffusion-limited, and assuming that the solution resistance had completely been compensated [179], the admittance is described as a parallel combination of a capacitor and a Warburg impedance:

$$Y = j\omega C + \frac{\sqrt{j\omega}}{\sigma'} \tag{4.2}$$

and the capacitance given as [269]:

$$C = (Y'' - Y')/\omega \tag{4.3}$$

where $\omega$ is the angular frequency, $Y$" and $Y$' are the imaginary and the real components of the admittance, respectively, and $\sigma$' is the Warburg diffusion coefficient.

In order to understand the measured capacitance curves, the interfacial region was modelled as a combination of three layers in series as described in section 2.9.3 and Figure 2.8. Similar equations to calculate the capacitance curves were also

employed in this work, however slight modifications were introduced, which are considered next. In the case of 2:1 electrolytes, the electric potential distribution in the region $x > 0$, is described by (publications I):

$$\frac{d^2\varphi}{dx^2} = \kappa_w^2 \left[ e^{\varphi - \Delta_o^w \varphi} - e^{-2(\varphi - \Delta_o^w \varphi)} \right] \tag{4.4}$$

$\varphi$ is the electric potential in $RT/F$ units and measured with respect to the bulk organic phase, and $\Delta_o^w \varphi$ is the dimensionless electrical potential in the bulk aqueous phase; the other symbols have the same meaning as described previously. The surface charge density $\sigma$, at the interface ($x = 0$), is considered as a sum of the contribution of the charge ($z$) of the phospholipid headgroups, the adsorbed calcium ions, and the adsorbed DS chains, and is given by:

$$\sigma = \frac{e}{A}[z_{headgroups} + 2\alpha - \beta] \tag{4.5}$$

$e$ is the elementary charge, $\alpha$ the degree of binding of $Ca^{2+}$ to any of the negatively charged oxygen radicals, and $\beta$ is a fitting parameter associated with the DS adsorbed chains. The interfacial charge density was evaluated from equation 4.6:

$$Q \equiv -\int_{-\infty}^{0} \rho dx = \frac{2\epsilon_0 RT}{F} \times [(\kappa_o^2 \epsilon_o^2 - \kappa_{hc}^2 \epsilon_{hc}^2) sinh^2(\varphi(-d_{hc})/2) + \kappa_{hc}^2 \epsilon_{hc}^2 sinh^2(\varphi(0)/2)]^{1/2} \tag{4.6}$$

(Equation 4.6 was incorrectly written in publications I and II, although the results reported are correct and were not affected by this typographical error). All the trends observed in the measured capacitance curves were explained by the theoretical model.

Inspection of the measured and calculated capacitance curves obtained in publication I for the lipid monolayer modified with DS showed that $Ca^{2+}$ bound to

DPPC created a positive interfacial charge density, and therefore, shifted the capacitance minimum towards more negative potentials. When the surface pressure was increased, the decrease of the effective $\epsilon_{hc}$ led to a decrease in the capacitance minimum. Adsorbed DS both shifted the minimum to more positive potentials and lowered the capacitance minimum, and increased the capacitance at negative potentials to values higher than at the bare interface. This was interpreted to be due to the adsorption of negatively charged DS chains. Also, the surface pressure increase decreased both the parameter $\beta$ and the effective $\epsilon_{hc}$. For the latter case, the result was equivalent to an increase in the thickness of the hydrocarbon region, similar to that observed by ellipsometric measurements when DS was added to zwitterionic lipid monolayers [105].

In the case of DPPA, similar trends in the capacitance data were observed. However, in the absence of DS, the shift of the capacitance minimum was to more positive potentials, and $Ca^{2+}$ bridges seemed to dominate over entropic effects at pressures lower than 60 mN/m, i.e. an increase in pressure led to higher concentrations of these bridges and, thus, to a better adsorption of DS. As a consequence, $\beta$ increased. Interestingly, at a surface pressure of 60 mN/m, the parameter $\beta$ decreased and led to desorption of DS chains. Furthermore, the parameter $\beta$ showed a non-monotonic trend in the case of DPPA, while for DPPC, the entropic effects seemed to be more important than electrostatic interactions at increasing surface pressures. As a result, DS chains were released, and $\beta$ decreased monotonically.

Interfacial capacitance was also used to characterise the LbL self-assembly of composite nanostructures containing a cationic polyelectrolyte (poly(allylamine hydrochloride) (PAH)) and negatively charged MSA-AuNPs at an aqueous/organic gel interface, where an anchoring layer of DOTAP monolayer modified with DS had previously been deposited (Figures 4.3a, publication II). In this study, AuNPs with two different size distribution were used, with average diameters of 1.7 and 2.9 nm.

The growth of the alternating PAH/AuNP multilayer films was followed with UV-vis spectroscopy. The spectra of the multilayers showed an almost linear increase in absorbance with the number of layers. It was suggested that the multilayers were

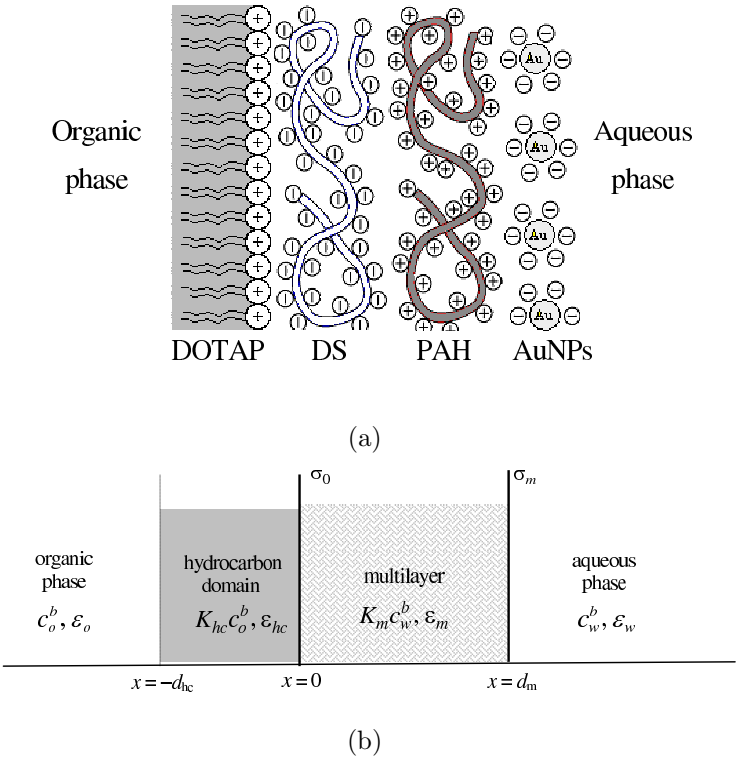


**Figure 4.3.** (a) Schematic representation of DOTAP/DS/PAH/AuNPs interfacial composite nanostructure. (b) Simplified view of the interfacial system as a four layer system at the ITIES. Reprinted with permission from publication II. Copyright © (2005) American Chemical Society.

assembled uniformly, each layer containing about the same amount of AuNPs. For the interpretation of the capacitance curves, a similar theoretical model to that described in section 2.9.3 was also used, but modified to account for the presence of DS and PAH/AuNP multilayers at the interface (Figure 4.3b). In this refined model, the composite DOTAP/DS/PAH/AuNP multilayers was modelled as a single phase that occupied the region $0 < x < d_m$ with a relative permittivity $\epsilon_m$, whereas the charges bound to the interfacial nanostructure, $\sigma_0$ and $\sigma_m$, were modelled as two plane distributions at $x = 0$ and $x = d_m$, respectively. Outside the multilayer, the interfacial system was modelled with the GC approach.

From the measured capacitance curves (Figure 4.4A) and those calculated using the theoretical model (Figure 4.4B), it was shown that the decrease of the overall capacitance with the number of layers was due to the increasing thickness as well as

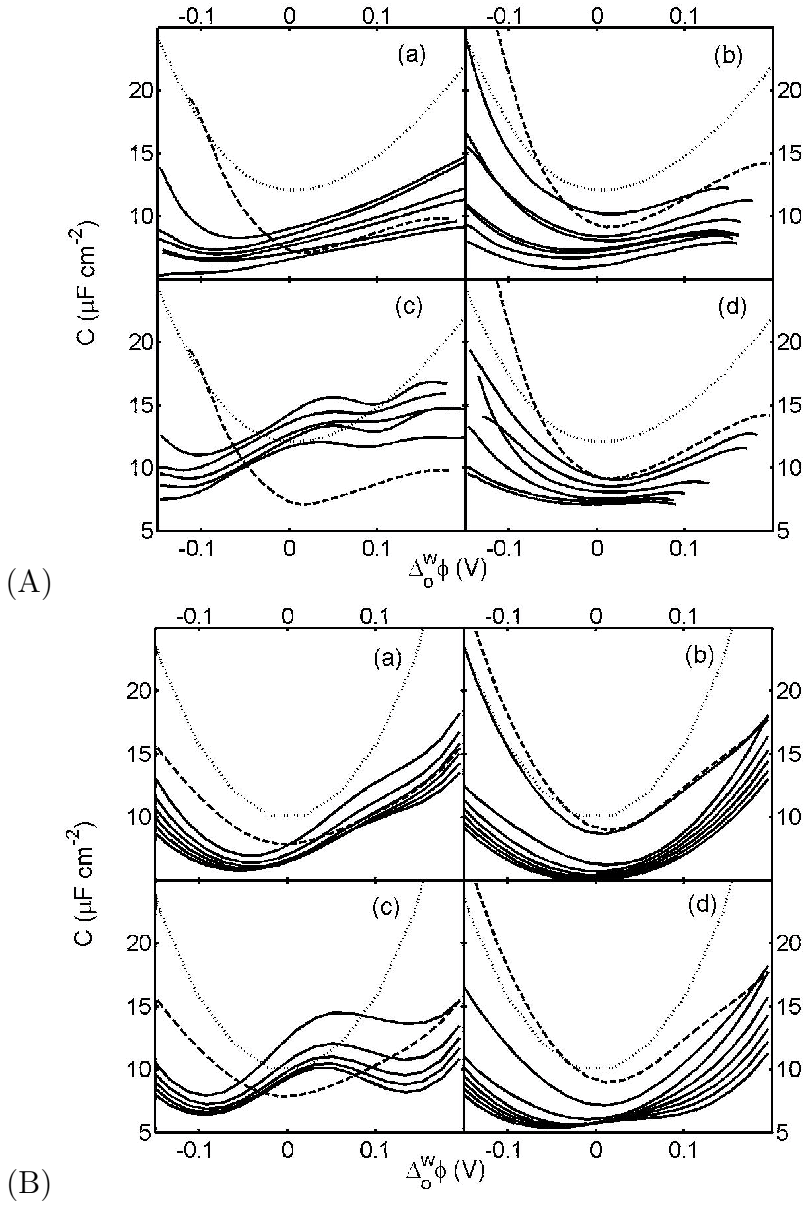


**Figure 4.4.** Experimental (A) and calculated (B) capacitance curves for multilayers containing 1.7 (a and b) and 2.9 nm AuNPs (c and d): (a, c) $n$ = odd layers (solid lines from top to bottom); (b, d) DOTAP/DS monolayer (dashed line) and $n$ = even layers (solid lines from top to bottom). Reprinted with permission from publication II. Copyright © (2005) American Chemical Society.

the decreasing partition coefficients of the supporting electrolytes in the hydrocarbon region and the multilayer. The potential of the capacitance minimum shifted to more negative values for PAH-terminated MLs while the contrary was observed

for AuNPs-terminated ones. Moreover, it was observed that these nanocomposites behaved similarly to polyelectrolyte multilayers, with the outmost layer determining the multilayer charge. Interestingly, the value of the outer charge density was much larger than that of the cationic phospholipids, increasing with the size and charge of the AuNPs.

Interfacial capacitance was employed to study the interactions between phospholipid monolayers and self-assembled DS-modified Ru NPs (publication III), and between mixed lipid/gA monolayers and DS (publication IV). In publication III, the charge distribution in the interfacial nanostructures formed by the phospholipid monolayers and adsorbed composite nanoclusters was elucidated using the theoretical model. The capacitance curves were successfully explained and were ascribed to a reduced surface charge density at the interface after the adsorption of the composite nanoclusters. Moreover, it was shown that the interactions were strongly dependent on the nature of the phospholipid headgroup, as stated in publication II. In general, as the surface pressure increased, the added nanoclusters decreased the capacitance minimum (indicated by the lower $\epsilon_{hc}$), and shifted it to more negative potentials (indicated by an increase in $\alpha$). Publication IV presented a different approach to mimic the biomembrane, where hybrid lipid/gA monolayers were modified by the addition of DS to an aqueous subphase containing $Ca^{2+}$ ions. It was shown that the DS chains form a rather flat and compact layer when adsorbed to either POPC or POPG monolayers. The importance of $Ca^{2+}$ ions in these interactions was also elucidated, and it was demonstrated that $Ca^{2+}$ interacts with gA channels even at low concentrations of gA in the lipid monolayers.

EIS was also used to study GOx/DPPC (or DBPC) interactions at a 1,2–DCE/water interface. The lipids were added to the organic phase and GOx to the aqueous phase. The experimental results were interpreted with the help of a model extended from the models above. GOx induced changes in the capacitance curves at both negative and positive potentials, which was ascribed to a reduced partition coefficient of the aqueous ions in the adsorbed layer as well as to an increase of the relative permittivity of the lipid hydrocarbon domain. The results emphasised

that lipid molecules enhanced the adsorption of GOx molecules at the liquid/liquid interface. At low lipid concentrations, the adsorption of GOx was probably the first step, preceding its penetration into the lipid monolayer, while at high GOx concentrations, the formation of GOx multilayers was observed. Lipids with longer carbon chains (DBPC) formed stable monolayers and were easily penetrated by GOx.

## 4.3 Synthesis, characterisation and properties of nanoparticles (II, III)

Since the properties of nanosized particles depend strongly on their size, shape and charge, they must be characterised adequately prior to their use. In this work, NPs were characterised with UV-Vis spectroscopy, which provides information about their optical properties, TEM, which provides information about their size distribution, shape and morphology, and zeta($\zeta$)-potential which provides information on their surface charge.

In order to study polyelectrolyte/AuNP multilayer films (publication II), water-soluble MSA-AuNPs were synthesised in aqueous medium as described by Chen and Kimura [204]. Basically, AuNPs with different sizes were obtained using different S/Au ratios. The S/Au ratio of 0.5 led to NPs with bigger sizes than the ratio 2.5. In the former case, AuNPs with an average diameter size of 2.9 nm were obtained, while in the latter case, the average diameter was 1.7 nm. The AuNPs synthesised according to this procedure are showed in Figure 4.5A. Large-sized particles appeared to be stable, while small-sized particles were difficult to observe even at very weak electron beam radiation. UV-vis was also employed to characterise the AuNPs. Small particles showed no adsorption peak in the spectra and a typical broad surface plasmon band appeared with bigger ones.

A novel nanostructure system, self-assembled from positively charged Ru NPs and negatively charged DS was prepared in an aqueous solution. The NPs were prepared under rigorous pH controlled conditions following the procedure described

by Yang [215]. The TEM images of the composite nanoclusters (Figure 4.5B) showed smooth spherical particles with an average diameter of about 40 nm, where the Ru NPs with a size of about 1.6 nm were surrounded by DS. ζ-potential of these nanoclusters were measured and an average value of about –36 mV was obtained, which indicates negative charge, proving that the DS chains were on the surface of the Ru NPs. The larger clusters observed in the TEM images were obtained in the presence of $Ca^{2+}$.

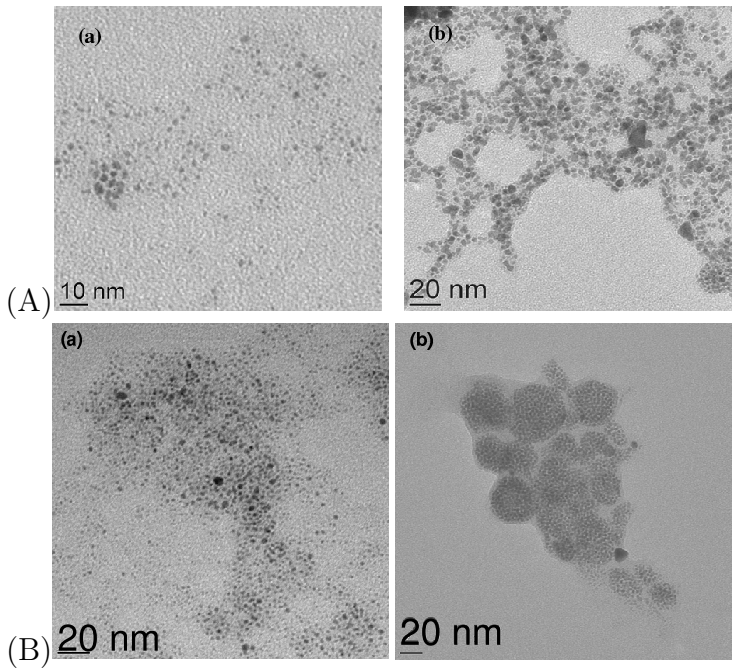


**Figure 4.5.** (A) TEM images of AuNPs of average diameter of 1.7 (a) and 2.9 nm (b). (B) TEM images of Ru NPs (unpublished result) (a) and composite nanoclusters (DS-modified Ru NPs) (b), with an average size diameter of 1.6 and 40 nm, respectively. Reprinted with permission from publication III. Copyright © (2007) Elsevier B. V.

## 4.4 Effect of the modified lipid monolayers on ion or drug transfer (I–IV)

In order to study the structural integrity of the model membranes and their ability to block or allow charge transfer, ion transfer was investigated with cyclic voltammetry and admittance measurements.

### 4.4.1 Cyclic voltammetry and admittance measurements

In cyclic voltammograms, an increase in the current at about $\Delta_o^w\phi$ = –0.1 V was observed, which indicates the adsorption of DS to DPPA monolayers (publication I). This current was less perceptible at surface pressures < 60 mN/m, and was almost absent when DS adsorbed to DPPC monolayers, which supported the ac voltammetry results.

In publication I, the transfer of probe ions, $TEA^+$ and metoprolol, was found to be under mixed kinetic and diffusion control. The CVs observed showed a peak separation of about 61 mV or higher, and therefore the apparent rate constants were calculated according to the Nicholson's method [186]. Interestingly, the results revealed that the transfer was slightly faster for monolayers modified with DS than for pure lipid monolayers, and it was suggested that lipid/$Ca^{2+}$/DS complexes could even to some extent facilitate the transfer.

Cyclic voltammetry was also employed to investigate the effect of the DOTAP/DS/PAH/AuNPs multilayer films on the transfer of the same molecules (publication II). The NP size significantly influenced the CV response, with a larger peak separation observed for multilayers containing 2.9 nm AuNPs. The rate of transfer observed for the multilayers system was slightly enhanced by the introduction of AuNPs in the multilayer, relative to those observed for polyelectrolyte/polyelectrolyte multilayers [221].

In publication III, the CVs for the transfer of two cationic drug molecules, aminacrine and tacrine, across POPC or POPG/$Ca^{2+}$/DS-modified Ru NPs showed that the drug molecules were also adsorbed on both the nanoclusters and the lipid

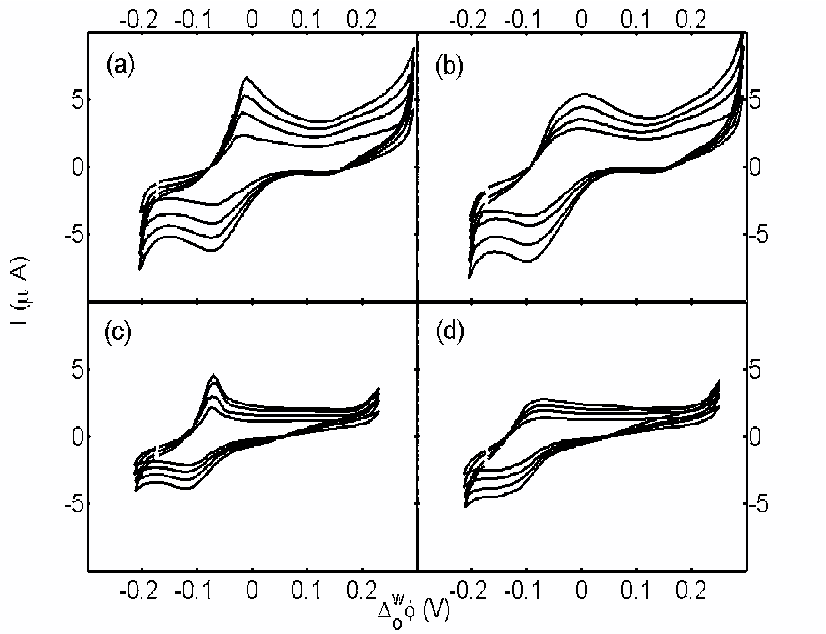


**Figure 4.6.** CVs of aminacrine (a, c) and tacrine (b, d) transfer recorded in the absence (a, b) and presence of POPC monolayers deposited at a surface pressure of 40 mN/m in the presence of composite nanoclusters. Reprinted with permission from publication III. Copyright © (2007) Elsevier B. V.

monolayer. The CVs of Figure 4.6 show an atypical shape of the forward peaks. These peaks were interpreted to be due to mixed adsorption, kinetics, and diffusion control of the transfer process. Furthermore, it was calculated that the lipid layer retarded the rate ion transfer by a factor of 2/3 and 1/2 for aminacrine and tacrine, respectively.

To elucidate the kinetics and mechanistic details of transfer, a more sensitive ac voltammetry technique was employed in publication IV, and the results were analysed with a theoretical mode. The model was previously used successfully to study the membrane activity [178,179], i.e. the tendency of a compound to interact with a biological membrane. The adsorption of electroactive species at the ITIES in connection with ac impedance/voltammetry has been treated by Samec [185] without assuming a specific isotherm or potential dependence of the rate constants. Following this work, a model was recently derived for adsorption of electroactive

species at a liquid/liquid interface which combined Bulter–Volmer description of the ion transfer kinetics with the possibility of specific adsorption both at the aqueous and organic sides of the interface [179].

The admittance data for the ion transfer showed that the electrical potential distribution and the chemical nature of the interface was strongly influenced by the presence of $Ca^{2+}$ in the subphase and gA in the lipid monolayer. Furthermore, it was observed that all ions adsorbed more strongly on the organic side of the interface and interacted preferentially with the hydrocarbon region of the lipid monolayers.

## 4.5 Binding of drug molecules to glycosaminoglycans (V)

A wide variety of molecules of pharmacological interest have surface active properties due to their amphiphilic nature. To achieve their target in the intracellular medium, their hydrophilic and hydrophobic moieties must firstly interact with the surface of the cellular membrane and its components. This interaction plays a fundamental role in biological phenomena. So far, approaches to investigate membrane interactions with amphiphilic drug molecules (such as propranolol, tacrine, and aminacrine) have been carried out by studying their interactions with lipids/liposomes and/or proteins (see section 2.11.2). In this work, particular attention was paid to the interaction of drug molecules with the surface components of a model membrane, such as GAGs.

Therefore, to get better insight on the binding between those drug molecules and GAGs, complementary ITC and fluorescence spectroscopy were used (publication V). Titration isotherms (Figure 4.7) were used to extract the thermodynamic parameters of binding between drugs and GAGs. In Figure 4.7, for the first few injections, tacrine was in large excess over the added GAG, and an almost constant heat release was observed. The plateau region reveals that the added GAG is bound completely to tacrine. As the titration continued (the concentration of GAG increases), the free drug concentration decreased, and the heat flow also decreased. Due to an increase in the endothermic contribution, the peaks suddenly decreased, and at higher GAG concentrations, no heat of interaction was observed.

The parameters $\Delta C_p$ and $\Delta S$ were further investigated using a method [250] that accounted for the hydrophobic and vibrational interactions between the GAG and drug molecules. Large negative values of $\Delta C_p$ were observed in the binding of GAGs to drugs, as a result of: (i) electrostatic forces, (ii) hydrophobic interaction between the apolar moieties, and (iii) possible GAG conformational changes. It was also highlighted that GAGs bind to drugs at one set of sites and that the electrostatic interactions between positively charged drugs and negatively charged GAGs may play an important role in the formation of drug/GAG complexes as a first step in the establishment of a hydrophobic interaction via aromatic ring stacking. Furthermore, the effect of the ionic strength and protonation/deprotonation on the binding enthalpy was also addressed. It was showed that the results were qualitatively independent of the buffer solution used. All these results were also supported by fluorescence measurements.

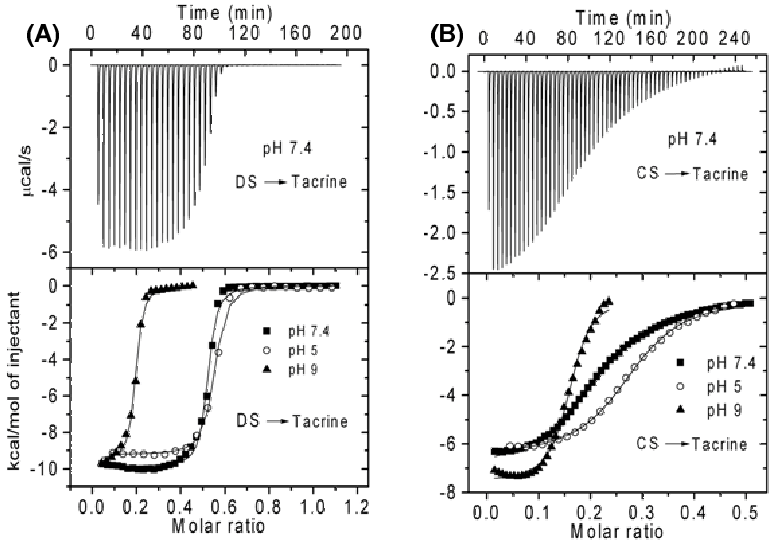


**Figure 4.7.** Calorimetric titrations of DS (A) and CS (B) into tacrine. The upper panels show the raw data and the lower ones show the plot of the total enthalpy exchanged as a function of the molar GAG/tacrine ratio. Reprinted with permission from publication V. Copyright © (2007) Elsevier B. V.

# 5 Conclusions and Outlook

The major aim of the thesis was to build more complex model membranes to study biological phenomena at a liquid/liquid interface. The model membrane was modified by the assembly of anionic GAGs (such as DS) and GOx on the polar phospholipid headgroups or by incorporation of gA into the phospholipid monolayer. Furthermore, the interactions between modified lipid monolayers, polyelectrolyte/AuNP multilayers and DS-modified Ru NPs were studied at a polarisable liquid/liquid interface. For that purpose, the LB technique was used to transfer the monolayers to a solid substrate. The membrane interactions with charged ions and therapeutic drugs were monitored using ac and dc electrochemical techniques. To obtain further information and explain the interfacial phenomena observed, theoretical models were developed. Finally, quantitative information on the binding between GAG and drug molecules were also assessed by ITC. The work presented here demonstrates that liquid/liquid electrochemistry is a powerful method to probe biological phenomena. The main conclusions of this thesis are given in the following section.

In the first publication, the interaction between lipid/$Ca^{2+}$/DS was analysed by means of electrochemical and FTIR techniques. The most important result was that, attractive electrostatic forces mediate lipid/$Ca^{2+}$/DS interactions. The presence of DS and $Ca^{2+}$ had a great influence on the physicochemical properties of the phospholipid monolayers. The interactions were strongly dependent on the packing and charge of the phospholipid monolayer. The complexation of the anionic DS chains with the lipid headgroups through calcium bridges and the partial ion exclusion from the hydrocarbon domain were the essential phenomena that explained the observed adsorption mechanism. DS adsorption also influenced the ion/drug transfer across the modified phospholipid monolayers. It was concluded that the addition of DS had two main effects: (i) it made the surface charge more negative (shifted the capacitance minimum to the right), and (ii) enhanced the concentration of small ions coming from the organic phase in the vicinity of the hydrophobic hydrocarbon tails. This led to a decrease of the dielectric constant, and thus higher capacitances

at negative potentials. The lipid/$Ca^{2+}$/DS interactions were strongly dependent on the surface pressure and applied potential, as well as on the phospholipid headgroup, in the case of the hybrid layer.

Subsequent work utilised phospholipid monolayers modified with DS to construct polyelectrolyte/AuNP (water-soluble) multilayers and mimic the ECM or the wall of controlled drug devices. The multilayer thickness, the partition coefficients of the supporting electrolyte in the hydrocarbon domain and multilayer, and the surface charge density were the most important parameters in the model used to explain the observed capacitance data. The polyelectrolyte/AuNP multilayers used to investigate ion transfer across the ITIES suggested that the ITIES can be successfully employed to optimise polyelectrolyte or metal NPs and multilayer formation conditions, and determine which is most appropriate for drug delivery systems. This system composed of complex biomimetic thin films (lipid + biopolymer + polyelectrolyte + NPs) can be used for constructing a biosensor for monitoring, for example, controlled-release and targeting sites of microcapsules in biological cells. For example, such capsules could be fabricated by the LbL technique by alternatively adsorbing oppositely charged polyelectrolytes on metal NPs, containing in their interior materials such as polymers, enzymes, drugs, etc., making them very suitable as potential delivery vesicles. The optimisation and manipulation of the surface charge and size of the AuNPs seem to be fundamental requirements for future developments on delivery processes.

In publication III, water-soluble and negatively charged DS/Ru NPs were prepared. Their interaction with phospholipid monolayers as well as their effect on drug transfer was investigated. The combination of DS and cationic Ru NPs via $Ca^{2+}$ bridges strongly interacted with the phospholipid monolayers, and affected the drug transfer across the liquid/liquid interface. The combination of positively charged NP surfaces and biomacromolecules can potentially be used for drug delivery systems. For example, in the system presented, a lipid monolayer serves as an in vitro model for a plasma membrane. Since the NPs also tune the permeability properties of the membranes, GAG-modified NPs are used in several drug formulations to tune

the release rate of the drug from the formulation. Therefore, this system mimics the interaction of such formulations with the plasma membrane. Moreover, NPs can be used to direct the formulation into the target tissue. This can be accomplished with a magnetic field if the NPs are magnetic. Ru NPs are not magnetic, but the catalytic properties of this or similar particles could be utilised in various redox reactions taking place in the tissues when in contact with a NP-containing formulation.

In publication IV, interactions between channel-forming gA and hybrid/gA monolayers with DS were described. The interactions observed varied according to the chemical nature of the lipid (hydrocarbon region and charge of the headgroup). It was concluded that the presence of $Ca^{2+}$ affected significantly the lipid/gA/DS interactions. Although drug molecules were not using gA channels to transfer through the lipid membranes due to their large size, it was demonstrated quantitatively that the transfer is a consequence of the modified surface charge as well as the thickness and compactness of the lipid/gA domain due to DS adsorption via calcium bridges at the interface. Ion transfer across the monolayer is possible, because gA binds lipid molecules tightly around itself, leaving a sparse lipid matrix elsewhere in the interface. This phenomenon is thought to be of great importance for biological and pharmacological permeability, since the ion transfer mechanism was very dependent on the membrane and subphase content, and therefore affecting the drug/membrane interactions, and consequently the regulation of drug transport.

The thermodynamic parameters of the interaction between positively charged drug molecules with negatively charged GAGs were determined in Publication V. As a result of the drug/GAG binding process, some information on drug delivery effects (facilitating or inhibiting) can be given. If the cell surface carries only a few GAGs, drug binding is limited to a few receptor molecules. In contrast, for a cell surface with a broad variety of GAGs, drug binding is nonselective. Adding a sufficient amount of drug, a neutral drug/GAG complex can be formed which, in turn, can be adsorbed to the membrane surface, facilitating either consecutive reactions steps or drug diffusion through the cell membrane. On the other hand,

adding relatively small amounts of drug, the complex will have an excess negative charge, and hence the complex is repelled from the membrane surface inhibiting drug transfer. Consequently, the formation of drug/GAG complexes seems to have an important role as a primary step for the drug delivery process into cell membranes, and should be taken into account when new drugs are designed. For example, the thermodynamic parameters determined by ITC may provide a qualitative readout for the thermodynamic effects of altering lead compound structures and may increase the success rate in structure-based drug design and/or optimisation. Furthermore, it was suggested that the results observed can be further used to regulate and improve the drug transport through the cell membrane.

Finally, in publication VI, the adsorption–penetration process of GOx into phospholipid monolayers was studied. Hydrophobic interactions were considered to play an important role in the formation of the mixed films, and contribute to the enzyme penetration into the organic phase to a considerable extent.

Conclusively, the addition of GAGs, gA, and GOx to phospholipid monolayers, may provide interesting and more complex models for biological membranes, which can be used to study specific interactions. Knowledge of membrane structure, composition and dynamics is very important to understand biological phenomena and their functions. Therefore, it is expected that the information given in this thesis can be further extended to *in vivo* studies, and open new ways of addressing biological phenomena from a bio-electrochemical point of view.

# List of Abbreviations

| | |
|---|---|
| *ac* | alternating current |
| *AFM* | atomic force microscopy |
| *ATR* | attenuated total reflection |
| *CS* | chondroitin sulfate |
| *CV(s)* | cyclic voltammogram(s) |
| *EIS* | electrochemical impedance spectroscopy |
| *ECM(s)* | extracellular matrix (matrices) |
| *DBPC* | dibehenoylphospatidylcholine |
| *dc* | direct current |
| *1,2–DCE* | 1,2–dichloroethane |
| *DmS* | dermatan sulfate |
| *DOPC* | dioleylphosphatidylcholine |
| *DOTAP* | dioleoyloxy-propyl-trimethylammomium chloride |
| *DPPA* | dipalmitoylphosphatidic acid |
| *DPPC* | dipalmitoylphosphatidylcholine |
| *DPPE* | dipalmitoylphosphatidylethanolamine |
| *DS* | dextran sulfate |
| *DSPC* | distearoylphosphatidylcholine |
| *FAD* | flavin adenine dinucleotide |
| *FTIR* | Fourier transform infrared |
| *gA* | gramicidin A |
| *GAG(s)* | glycosaminoglycan(s) |
| *GC* | Gouy–Chapman |
| *GlcA* | glucuronic acid |
| *GOx* | glucose oxidase |
| *HA* | hyaluronan/hyaluronic acid/hyluronate |
| *HS* | heparan sulfate |

| | |
|---|---|
| *ITC* | isothermal titration calorimetry |
| *ITIES* | interface between two immiscible electrolytes |
| *KS* | Keratan sulfate |
| *LbL* | layer-by-layer |
| *LDL(s)* | low-density lipoprotein(s) |
| *LB* | Langmuir–Blodgett |
| *LC* | liquid–condensed phase |
| *LE* | liquid–expanded phase |
| *MSA* | mercaptosuccinic acid |
| *MVN* | modified Verwey–Niessen model |
| *NMR* | nuclear magnetic resonance |
| *NP(s)* | nanoparticle(s) |
| *ODA* | octadecylamine |
| *o-NPOE* | o-nitrophenyloctylether |
| *PA* | phosphatidic acid |
| *PAH* | poly(allylamine hydrochloride) |
| *PB* | Poisson–Boltzman |
| *PC* | phosphatidylcholine |
| *PE* | phosphatidylethanolamine |
| *PEI* | polyethylenimine |
| *PG(s)* | proteoglycan(s) |
| *PI* | phosphatidylinositol |
| *PLYS* | poly(L-lysine) |
| *PM-FTIR* | polarisation modulation Fourier transform infrared |
| *POPC/POPG* | palmitoyloleoyl-phosphatidylcholine/phosphoglycerol |
| *PS* | phosphatidylserine |
| *PVC* | poly(vinyl chloride) |
| *SECM* | scanning electrochemical microscopy |

| | |
|---|---|
| $SM$ | sphingomyelin |
| $STM$ | scanning tunnelling microscopy |
| $TEA^+$ | tetraethylammonium cation |
| $TEM$ | transmission electron microscopy |

# List of Symbols

| | |
|---|---|
| $A$ *or* $A_L/mmA$ | surface area or mean molecular area of the lipid |
| $A_{gA}$ | mean molecular area of gramicidin A |
| $a_i^o/a_i^w$ | activities of ion $i$ in water or organic phase |
| $C$ ($C_{dl}$) | capacitance (double-layer) |
| $C_s^{-1}$ | compressibility modulus |
| $c_i^b$ | concentration of species $i$ in aqueous or organic bulk phases |
| $D_w/D_o$ | diffusion coefficient of the transferring ion in water or organic phase |
| $F$ | Faraday constant |
| $k^0$ | standard rate constant |
| $k_f$ | forward rate constant |
| $k_b$ | backward rate constant |
| $K_b$ | binding constant |
| $K_{hc}$ | chemical partition coefficient of the organic electrolyte between the hydrocarbon region and the bulk organic phase |
| $Q$ | surface charge density |
| $Q_i$ | charge in the phase $i$ |
| $R_{ct}$ | charge transfer resistance |
| $T$ | absolute temperature |
| $W$ | Warburg impedance |
| $X_L$ | molar fraction of the lipid |
| $Y$ | total admittance |
| $Y'/Y''$ | real and imaginary component of a measured total admittance |
| $Z'/Z''$ | real and imaginary impedance |
| $z_i$ | charge number of ion ($i$) |
| | |
| $\alpha$ | apparent charge transfer coefficient or the degree of binding of $Ca^{2+}$ |
| $\beta$ | fitting parameter associated to the dextran sulfate adsorbed chains |
| $\Delta C_p$ | heat capacity |

| | |
|---|---|
| $\Delta H$ | binding enthalpy |
| $\Delta G$ | Gibbs free energy |
| $\Delta S$ | entropy |
| $\Delta G_{i,tr.}^{w \longrightarrow o}$ | Gibbs free energy of transfer of species $i$ |
| $\Delta_o^w \phi$ | Galvani potential difference between water and organic phase |
| $\Delta_o^w \phi_i^0$ | standard transfer potential of the ion $i$ |
| $\Delta_o^w \phi_i^{0'}$ | formal transfer potential of the ion $i$ |
| $\Delta_o^w \varphi$ | dimensionless potential difference between the bulk aqueous and organic phases |
| $\epsilon_i^b$ | relative permittivities of the aqueous or organic bulk phases |
| $\epsilon_{hc}$ | relative permittivity of the hydrocarbon region |
| $\gamma$ | surface tension |
| $\kappa_i$ | reciprocal Debye length |
| $\mu_i^{0,o}/\mu_i^{0,w}$ | standard chemical potentials of ion $i$ in water or organic phase |
| $\omega$ | angular frequency |
| $\pi$ | surface pressure |
| $\psi$ | kinetic parameter |
| $\sigma$ | surface charge |
| $\sigma$ ' | Warburg diffusion coefficient |
| $\zeta$ | zeta(-potential) |

# References


[1] R. B. Gennis, *in*: Biomembranes: Molecular Structure and Function, C. R. Cantor (Ed.), Springer-Verlag, New York, 1989.

[2] M. C. Petty, Langmuit–Blodgett Films: An Introduction, University Press, Cambridge, 1996, pp. 13, 14.

[3] E. Sackmann, Phospholipid Monolayers, *in*: Structure and Dynamics of Membranes. From Cells to Vesicles, R. Lipowsky, E. Sackmann (Eds.), Vol. 1, Elsevier, Amsterdam, 1995, Ch. 4, pp. 1–63.

[4] C. M. Niemeyer, C. A. Mirkin, Nanobiotechnology, Wiley, 2004.

[5] E. Gorter, F. Grendel, *J. Exp. Med.* **41** (1925) 439–443.

[6] S. J. Singer, G. L. Nicolson, *Science* **175** (1972) 720–731.

[7] J. N. Israelachvili, *Biochim. Biophys. Acta* **469** (1977) 221–225.

[8] D. M. Engelman, *Nature* **438** (2005) 578–580.

[9] S. J. Crook, J. M. Boggs, A. I. Vistnes, K. M. Koshy, *Biochemistry* **25** (1986) 7488–7494.

[10] R. J. Stewart, J. M. Boggs, *Biochemistry* **32** (1993) 10666–10674.

[11] D. L. Nelson, M. M. Cox, *in*: Lehninger Principles of Biochemistry, E. Geller (Ed.), Vol. III, Worth Publishers, NY, USA, 2000.

[12] S. Scarlata, *Biophys. Chem.* **69** (1997) 9–21.

[13] D. D. Chiras, Human Biology, 5th Edition, Jones & Bartlett Publishers, New York, 2005.

[14] J. M. Seddon, R. H. Templer, Polymorphism of lipid-water systems, *in*: Structure and Dynamics of Membranes. From Cells to Vesicles, R. Lipowsky, E. Sackmann (Eds.), Vol. 1, Elsevier, Amsterdam, 1995, pp. 97–160.

[15] A. H. Vries, S. Yefimov, A. E. Mark, S. J. Marrink, *Proc. Natl. Acad. Sci. U.S.A.* **102** (2005) 5392–5396.

[16] O. G. Mouritsen, *in*: Life as a matter of fat: The Emerging Science of Lipidomics, D. Dragoman, M. Dragoman, A. C. Elitzur, M. P. Silverman, J. Tuszynski, H. D. Zeh (Eds.), Vol. 1, The Frontiers Collection-Springer, Germany, 2005.

[17] J. Mason, *Methods Enzymol.* **295** (1998) 468–494.

[18] R. Koynova, M. Caffrey, *Biochim. Biophys. Acta* **1376** (1998) 91–145.

[19] D. Marsh, *Biochim. Biophys. Acta* **1286** (1996) 183–223.

[20] R. S. Cantor, *Biochemistry* **36** (1997) 2339–2344.

[21] M. C. Morris, P. Vidal, L. Chaloin, F. Heitz, G. Divita, *Nucleic Acids Res.* **25** (1997) 2730–2736.

[22] N. V. Mau, V. Vié, L. Chaloin, E. Lesniewska, F. Heitz, C. L. Grimellec, *J. Membrane Biol.* **167** (1999) 241–249.

[23] F. Y. Chen, M. T. Lee, H. W. Huang, *Biophys. J.* **84** (2003) 3751–3758.

[24] M. Zasloff, *Nature* **415** (2002) 389–395.

[25] N. Y. Papo, Y. Shai, *Biochemistry* **42** (2003) 458–466.

[26] E. J. M. van Kan, D. E. Breukink, A. van der Bent, B. de Kruijff, *Biochemistry* **41** (2002) 7529–7539.

[27] M. Dathe, J. Meyer, M. Beyermann, B. Maul, C. Hoischen, M. Bienert, *Biochim. Biophys. Acta* **1558** (2002) 171–186.

[28] C. Whitehouse, D. Gidalevitz, M. Cahuzac, K. E. KoeppeII, A. Nelson, *Langmuir* **20** (2004) 9291–9298.

[29] O. S. Andersen, K. E. KoeppeII, B. Roux, *Cell. Mol. Life Sci.* **63** (2006) 301–315.

[30] K. E. KoeppeII, O. S. Andersen, *J. Biol. Chem.* **269** (1994) 1934–1939.

[31] B. Hille, Ionic Channels of Excitable Membranes, Sinauer Associates, Sunderland, MA, 1992.

[32] W. Jing, Z. Wu, E. Wang, *Electrochim. Acta* **44** (1998) 99–102.

[33] S. Alonso-Romanowski, L. M. Gassa, J. R. Vilche, *Electrochim. Acta* **40** (1995) 1561–1567.

[34] C. A. Gervasi, A. E. Vallejo, *Electrochim. Acta* **47** (2002) 2259–2264.

[35] Y. Chen, B. A. Wallace, *Biophys. J.* **26** (1997) 299–306.

[36] B. Corry, S. H. Chung, *Cell. Mol. Life Sci.* **63** (2006) 301–315.

[37] R. R. Ketchem, T. Hu, T. A. Cross, *Science* **261** (1993) 1457–1460.

[38] K. E. KoeppeII, F. J. Sigworth, G. Szabo, D. Urry, A. Woolley, *Nat. Struct. Biol.* **6** (1999) 609.

[39] T. A. Cross, A. Arseniev, B. A. Cornell, J. H. Davis, J. A. Killian, K. E. KoeppeII, L. K. Nicholson, F. Separovic, B. Wallace, *Nat. Struct. Biol.* **6** (1999) 610–611.

[40] B. M. Burkhart, W. L. Daux, *Nat. Struct. Biol.* **6** (1999) 611–612.

[41] J. A. Killian, *Biochim. Biophys. Acta* **1113** (1992) 391–425.

[42] J. Mauzeroll, M. Buda, A. J. Bard, F. Prieto, M. Rueda, *Langmuir* **18** (2002) 9453–9461.

[43] S. Fahsel, E.-M. Pospiech, M. Zein, T. L. Hazlet, E. Gratton, R. Winter, *Biophys. J.* **83** (2002) 334–344.

[44] A. Nelson, *J. Electroanal. Chem.* **303** (1991) 221–236.

[45] H. Takeuchi, Y. Nemoto, I. Harada, *Biochemistry* **29** (1990) 1572–1579.

[46] K. E. KoeppeII, J. A. Killian, D. V. Greathouse, *Biophys. J.* **66** (1994) 14–24.

[47] S. A. Seoh, D. Busath, *Biophys. J.* **68** (1995) 2271–2279.

[48] T. Maruyama, H. Takeuchi, *Biochemistry* **36** (1997) 10993–11001.

[49] A. Finkelstein, O. S. Andersen, *J. Membr. Biol.* **39** (1981) 155–171.

[50] D.-G. Levitt, S. R. Elias, J. M. Hautman, *Biochim. Biophys. Acta* **512** (1978) 436–451.

[51] H. Tournois, P. Gieles, R. Demel, J. de Gier, B. de Kruijff, *Biophys. J.* **55** (1989) 557–569.

[52] J. A. Szule, R. P. Rand, *Biophys. J.* **85** (2003) 1702–1712.

[53] M. Diociaiuti, F. Bordi, A. Motta, A. Carosi, A. Molinari, G. Arancia, C. Coluzza, *Biophys. J.* **82** (2002) 3198–3206.

[54] V. L. Shapovalov, E. A. Kotova, T. I. Rokitskaya, Y. N. Antonenko, *Biophys. J.* **77** (1999) 299–305.

[55] C. Whitehouse, R. O'Flanagan, B. Lindholm-Sethson, B. Movaghar, A. Nelson, *Langmuir* **20** (2004) 136–144.

[56] G. Kim, M. Gurau, S.-M. Lim, P. S. Cremer, *J. Phys. Chem. B* **107** (2003) 1403–1409.

[57] D. Ducharme, D. Vaknin, M. Paudler, C. Salesse, H. Riegler, H. Möhwald, *Thin Solid Films* **284–285** (1996) 90–93.

[58] W.-P. Ulrich, H. Vogel, *Biophys. J.* **76** (1999) 1639–1647.

[59] H. Lavoie, D. Blaudez, D. Vaknin, B. Desbat, B. M. Ocko, C. Salesse, *Biophys. J.* **83** (2002) 3558–3569.

[60] A. Nelson, *J. Chem. Soc. Faraday Trans.* **87** (1991) 1851–1856.

[61] M. Rueda, I. Navarro, G. Ramirez, F. Prieto, C. Prado, A. Nelson, *Langmuir* **15** (1999) 3672–3678.

[62] M. Rueda, I. Navarro, C. Prado, C. Silva, *J. Electrochem. Soc.* **148** (2001) E139–E147.

[63] A. Nelson, *Biophys. J.* **80** (2001) 2694–2703.

[64] F. Prieto, I. Navarro, M. Rueda, *J. Electroanal. Chem.* **550–551** (2003) 253–265.

[65] D. A. Metzler, Biochemistry: The Chemical Reactions of Living Cells, 2nd Edition, Academic Press, California, 2003, p. 1153.

[66] C. I. Gama, L. C. Hsieh-Wilson, *Curr. Opin. Chem. Biol.* **9** (2005) 609–619.

[67] T. Laabs, D. Carulli, H. M. Geller, J. W. Fawcett, *Curr. Opin. Neurobiol.* **15** (2005) 116–120.

[68] I. Capila, R. J. Linhardt, *Angew. Chem. Int. Ed. Engl.* **41** (2002) 391–412.

[69] H. E. Bülow, O. Hobert, *Neuron.* **41** (2004) 723–736.

[70] J. Schlessinger, I. Lax, M. Lemmon, *M. Cell* **83** (1995) 357–360.

[71] K. Prydz, K. T. Dalen, *J. Cell Sci.* **113** (2000) 193–205.

[72] H. Lodish, A. Berk, L. Zipursky, P. Matsudaira, D. Baltimore, J. Darnell, Molecular Cell Biology, 4th Edition, W. H. Freeman, New York, 2000, Ch. 5.

[73] P. A. Brittis, D. R. Canning, J. Silver, *Science* **255** (1992) 733–736.

[74] M. Ruponen, S. Ylä-Herttuala, A. Urtti, *Biochim. Biophys. Acta* **1415** (1998) 1–12.

[75] M. Ruponen, P. Honkakoski, M. Tammi, A. Urtti, *J. Gene Med.* **6** (2004) 405–414.

[76] K. A. Mislick, D. Baldeschwieler, *Proc. Natl. Acad. Sci. USA* **93** (1996) 12349–12354.

[77] L. C. Mounkes, W. Zhong, G. Cipres-Palacin, R. J. Debs, *Science* **273** (1998) 26164–26170.

[78] B. Radhakrishnamurthy, H. A. Ruitz, S. R. Srinivasan, W. Preau, E. R., D. G. S. Berenson, *Atherosclerosis* **31** (1978) 217–229.

[79] A. D. Bangham, M. W. Hill, N. G. A. Miller, *Science* **240** (1988) 646–649.

[80] J. C. Mai, H. Shen, S. C. Watkins, T. Cheng, P. D. Robbins, *J. Biol. Chem.* **277** (2002) 30208–30218.

[81] W. Tiyaboonchai, J. Woiszwillo, R. C. Sims, C. R. Middaugh, *Int. J. Pharm.* **255** (2003) 139–151.

[82] W. Tiyaboonchai, J. Woiszwillo, C. R. Middaugh, *Int. J. Pharm.* **19** (2003) 191–202.

[83] G. Camejo, *Adv. Lipid Res.* **19** (1982) 1–53.

[84] T. Nishida, U. Cogan, *J. Biol. Chem.* **245** (1970) 4689–4697.

[85] P. Bernfeld, T. F. Kelley, *J. Biol. Chem.* **239** (1964) 3341–3346.

[86] T. Nishida, *J. Lipid Res.* **9** (1968) 627–635.

[87] P.-H. Iverius, *J. Biol. Chem.* **247** (1972) 2607–2613.

[88] Y. C. Kim, T. Nishida, *J. Biol. Chem.* **252** (1977) 1243–1249.

[89] Y. C. Kim, T. Nishida, *J. Biol. Chem.* **254** (1979) 9621–9626.

[90] S. R. Srinivasan, B. Radhakrishnamurthy, G. S. Berensonl, *Arch. Biochem. Biophys.* **170** (1975) 334–340.

[91] M. Krumbiegel, H. Machill, O. Zschörning, D. Wiegel, K. Arnold, *Studia Biophys.* **136** (1990) 71–80.

[92] A. Mitterer, W. D. Eigner, J. Schurz, G. Juergens, A. Holasek, *Int. J. Biol. Macromol.* **4** (1982) 227–232.

[93] G. Camejo, A. Lopez, F. Lopez, J. Quinones, *Atherosclerosis* **55** (1985) 93–105.

[94] L. L. Rudel, J. S. Parks, F. L. Johson, J. Babiak, *J. Lipid Res.* **28** (1986) 465–474.

[95] K. Arnold, S. Ohki, M. Krumbiegel, *Chem. Phys. Lipids* **55** (1990) 301–307.

[96] K. Arnold, J. Arnhold, O. Zschörning, D. Wiegel, K. M. Krumbiegel, *Biomed. Biochim. Acta* **48** (1989) 735–742.

[97] A. D. Cardin, H. J. R. Weintraub, *Arteriosclerosis* **9** (1989) 21–32.

[98] K. H. Weisgraber, S. C. Rall, *J. Biol. Chem* **262** (1987) 11097–11103.

[99] M. Krumbiegel, K. Arnold, *Chem. Phys. Lipids* **136** (1990) 71–80.

[100] G. Steffan, S. Wulff, H. J. Galla, *Chem. Phys. Lipids* **74** (1994) 141–150.

[101] D. B. Fenske, R. J. Cushley, *Chem. Phys. Lipids* **54** (1990) 9–16.

[102] D. Huster, K. Arnold, *Biophys. J.* **75** (1998) 909–916.

[103] M. Bihari-Varga, J. Sztatisz, S. Gal, *Atherosclerosis* **39** (1981) 10–23.

[104] D. Huster, G. Paasche, U. Dietrich, O. Zschörning, T. Gutberlet, K. Gawrisch, K. Arnold, *Biophys. J.* **77** (1999) 879–887.

[105] K. de Meijere, G. Brezesinski, O. Zschörning, K. Arnold, H. Möhwald, *Physica B* **248** (1998) 269–273.

[106] K. de Meijere, G. Brezesinski, H. Möhwald, *Macromolecules* **30** (1997) 2337–2342.

[107] T. Akesson, C. E. Woodward, B. Jönsson, *J. Chem. Phys.* **91** (1989) 2461–2469.

[108] R. Podgornik, *J. Phys.Chem.* **95** (1991) 5249–5255.

[109] R. Podgornik, *J. Phys.Chem.* **96** (1992) 884–896.

[110] D. Huster, U. Dietrich, T. Gutberlet, K. Gawrisch, K. Arnold, *Langmuir* **16** (2000) 9225–9232.

[111] D. G. Georganopoulou, D. J. Caruana, J. Strutwolf, D. E. Williams, *Faraday Discuss.* **16** (2000) 109–118.

[112] H. J. Hecht, H. M. Kalizs, J. Hendle, R. D. Schmid, D. Schomburg, *J. Mol. Biol.* **229** (1993) 153–172.

[113] H. J. Hecht, D. Schomburg, H. M. Kalizs, R. D. Schmid, *Biosens. Bioelectron.* **8** (1993) 197–203.

[114] A. Baszkin, M. M. Boissonnade, V. Rosilio, A. Kamyshny, S. Magdassi, *J. Colloid Interface Sci.* **209** (1999) 302–311.

[115] http://www-biol.paisley.ac.uk/marco/enzyme(underscore)electrode/chapter3/chapter3(underscore)page4.htm.

[116] D. G. Georganopoulou, D. E. Williams, C. M. Pereira, F. Silva, T. Su, J. R. Lu, *Langmuir* **19** (2003) 4977–4984.

[117] S. Sun, P. H. Ho-Si, D. J. Harrison, *Langmuir* **7** (1991) 727–737.

[118] J. Rinuy, P. F. Brevet, H. H. Girault, *Biophys. J.* **77** (1999) 3350–3355.

[119] V. Rosilio, M. M. Boissonnade, J. Zhang, L. Jiang, A. Baszkin, *Langmuir* **13** (1997) 4669–4675.

[120] Y.-K. Du, J.-Y. An, J. Tang, Y. Li, L. Jiang, *Colloids Surf. B* **7** (1996) 129–133.

[121] J. Zhang, V. Rosilio, M. M. B. M. Goldmann, A. Baszkin, *Langmuir* **16** (2000) 1226–1232.

[122] J. Li, V. Rosilio, M. M. Boissonnade, A. Baszkin, *Colloid Surf. B* **29** (2003) 13–20.

[123] B. Franklin, *Phil. Trans. R. Soc. London* **64** (1774) 445.

[124] I. Langmuir, *J. Am. Chem. Soc.* **39** (1917) 1848–1906.

[125] K. B. Blodgett, *J. Am. Chem. Soc.* **57** (1935) 1007–1022.

[126] H. Möhwald, Phospholipid Monolayers, *in*: Structure and Dynamics of Membranes. From Cells to Vesicles, R. Lipowsky, E. Sackmann (Eds.), Vol. 1, Elsevier, Amsterdam, 1995, Ch. 4, p. 164.

[127] J. Als-Nielsen, D. Jacquemain, K. Kjaer, F. Leveiller, M. Lahav, L. Leiserowitz, *Physics Reports* **246** (1994) 251–313.

[128] J. Israelachvili, *Langmuir* **10** (1994) 3774–3781.

[129] V. B. Fainerman, D. Vollhardt, V. Melzer, *J. Phys. Chem.* **100** (1996) 15478–15482.

[130] V. M. Kaganer, H. Möhwald, P. Dutta, *Rev. Mod. Phys.* **71** (1999) 779–819.

[131] H. Brockman, *Curr. Opin. Struct. Biol.* **9** (1999) 438–443.

[132] V. M. Säily, S. Ryhänen, J. H. Holopainen, S. Borocci, G. Mancini, P. K. J. Kinnunen, *Biophys. J.* **81** (2001) 2135–2143.

[133] V. M. Säily, J.-M. Alakoskela, S. Ryhänen, M. Karttunen, P. K. J. Kinnunen, *Langmuir* **19** (2003) 8956–8963.

[134] J. H. Brooks, B. A. Pethica, *Trans. Faraday Soc.* **60** (1964) 208–215.

[135] B. Y. Yue, C. M. Jackson, J. A. Taylor, J. Mingins, B. A. Pethica, *J. Chem. Soc. Faraday Trans. I* **72** (1976) 2685–2693.

[136] J. A. Taylor, J. Mingins, B. A. Pethica, *J. Chem. Soc. Faraday Trans. I* **72** (1976) 2694–2702.

[137] M. C. Phillips, D. Chapman, *Biophys. Acta* **163** (1968) 301–313.

[138] J. Mingins, J. A. Taylor, B. A. Pethica, C. M. Jackson, B. Y. T. Yue, *J. Chem. Soc. Faraday Trans. I* **82** (1982) 323–339.

[139] M. Thoma, H. Möhwald, *J. Colloid Interface Sci.* **162** (1994) 340–349.

[140] G. Brezesinski, M. Thoma, B. Struth, H. Möhwald, *J. Phys. Chem.* **100** (1996) 3126–3130.

[141] H. M. McConnell, L. K. Tamm, R. M. Weis, *Proc. Natl. Acad. Sci. USA* **81** (1984) 3249–3253.

[142] M. Lösche, H.-P. Duwe, H. Möhwald, *J. Colloid Interface Sci.* **126** (1988) 432–444.

[143] M. Flörsheimer, H. Möhwald, *Colloid Surf.* **55** (1991) 173–189.

[144] C. A. Helm, H. Möhwald, K. Kjær, J. Als-Nielsen, *Europhys. Lett.* **4** (1987) 697–703.

[145] M. B. Forstner, J. Käs, D. Martin, *Langmuir* **17** (2001) 567–570.

[146] B. Gabriel, J. Teissié, *J. Am. Chem. Soc.* **113** (1991) 8818–8821.

[147] J. Zhang, P. R. Unwin, *J. Am. Chem. Soc.* **124** (2002) 2379–2383.

[148] S. Cannan, J. Zhang, F. Grunfeld, P. R. Unwin, *Langmuir* **20** (2004) 701–707.

[149] T. Kakiuchi, M. Kotani, J. Noguchi, M. Nakanishi, M. Senda, *J. Colloid Interface Sci.* **149** (1992) 279–289.

[150] J. Koryta, L. Q. Hung, A. Hofmanová, *Studia Biophys.* **90** (1982) 25–29.

[151] V. J. Cunnane, D. J. Schiffrin, M. Fleischmann, G. Geblewicz, D. Williams, *J. Electroanal. Chem.* **243** (1988) 455–464.

[152] A.-K. Kontturi, K. Kontturi, L. Murtomäki, V. J. Cunnane, *J. Electroanal. Chem.* **424** (1997) 69–74.

[153] D. Grandell, L. Murtomäki, *Langmuir* **14** (1998) 556–559.

[154] Y. Cheng, D. J. Schiffrin, *J. Chem. Soc. Faraday Trans.* **90** (1994) 2517–2523.

[155] M. Tsionsky, A. J. Bard, M. V. Mirkin, *J. Am. Chem. Soc.* **119** (1997) 10785–10792.

[156] A. Watanabe, A. Fujii, Y. Sakamori, K. Higashitsuji, H. Tamai, *Kolloid-Z. Z. Polym.* **243** (1971) 42–47.

[157] A. Watanabe, M. Matsumoto, H. Tamai, R. Gotoh, *Kolloid-Z. Z. Polym.* **228** (1968) 58–63.

[158] H. H. Girault, D. J. Schiffrin, *J. Electroanal. Chem.* **179** (1984) 277–284.

[159] T. Kakiuchi, M. Yamme, T. Osakai, M. Senda, *Bull. Chem. Soc. Jpn.* **60** (1987) 4223–4228.

[160] T. Kakiuchi, T. Kondo, M. Kotani, M. Senda, *Langmuir* **8** (1992) 169–175.

[161] T. Kakiuchi, T. Kondo, M. Senda, *Bull. Chem. Soc. Jpn.* **63** (1990) 3270–3276.

[162] T. Kakiuchi, M. Nakanishi, M. Senda, *Bull. Chem. Soc. Jpn.* **62** (1989) 403–409.

[163] T. Wandlowski, V. Mareček, Z. Samec, *J. Electroanal. Chem.* **242** (1988) 277–290.

[164] Z. Samec, A. Trojánek, H. H. Girault, *Electrochem. Commun.* **5** (2003) 98–103.

[165] H. H. J. Girault, D. J. Schiffrin, Charge Transfer Through Phospholipid Monolayers Adsorbed at Liquid/Liquid Interfaces, *in*: Charge And Effects in Biosystems., M. J. Allen, P. N. R. Usherwood (Eds.), Abacus Press, Tunbridge Wells, 1984, pp. 171–178.

[166] H. A. Santos, C. M. Pereira, F. Silva, *Port. Electrochim. Acta* **22** (2005) 263–274.

[167] M. C. Martins, C. M. Pereira, H. A. Santos, R. Dabirian, F. Silva, V. García-Morales, J. M. Manzanares, *J. Electroanal. Chem.* **599** (2007) 367–375.

[168] J. Koryta, *Electrochim. Acta* **24** (1979) 293–300.

[169] C. J. Slevin, S. Ryley, D. J. Walton, P. R. Unwin, *Langmuir* **14** (1998) 5331–5334.

[170] R. M. Allen, D. E. Williams, *Faraday Discuss.* **104** (1998) 281–293.

[171] D. Grandell, L. Murtomäki, K. Kontturi, G. Sundholm, *J. Electroanal. Chem.* **463** (1999) 242–247.

[172] S. G. Chesniuk, S. A. Dassie, L. M. Yudi, A. M. Baruzzi, *Electrochim. Acta* **43** (1998) 2175–2181.

[173] S. G. Chesniuk, S. A. Dassie, L. M. Yudi, A. M. Baruzzi, *Electrochim. Acta* **14** (1998) 5226–5230.

[174] J. A. Manzanares, R. M. Allen, K. Kontturi, *J. Electroanal. Chem.* **483** (2000) 188–196.

[175] D. Grandell, L. Murtomäki, G. Sundholm, *J. Electroanal. Chem.* **469** (1999) 72–78.

[176] J. Strutwolf, J. Zhang, A. L. Barker, P. R. Unwin, *Phys. Chem. Chem. Phys.* **3** (2001) 5553–5558.

[177] P. Liljeroth, A. Mälkiä, V. J. Cunnane, A.-K. Kontturi, K. Kontturi, *Langmuir* **16** (2000) 6667–6673.

[178] A. Mälkiä, P. Liljeroth, K. Kontturi, *Anal. Sci.* **17** (2001) i345–i348.

[179] A. Mälkiä, P. Liljeroth, A.-K. Kontturi, K. Kontturi, *J. Phys. Chem. B* **105** (2001) 10884–10892.

[180] A. Mälkiä, P. Liljeroth, K. Kontturi, *Electrochem. Commun.* **5** (2003) 473–479.

[181] A. Mälkiä, P. Liljeroth, K. Kontturi, *Chem. Commun.* (2003) 1430–1431.

[182] K. Kontturi, L. Murtomäki, *J. Pharm. Sci.* **81** (1992) 970–975.

[183] F. Reymond, P.-A. Carrupt, B. Testa, H. H. Girault, *Chem. Eur. J.* **5** (1999) 39–47.

[184] A. J. Bard, L. R. Faulkner, Electrochemical Methods, 2nd Edition, Wiley, 2001.

[185] Z. Samec, *J. Electroanal. Chem.* **426** (1997) 31–35.

[186] R. S. Nicholson, *Anal. Chem.* **37** (1965) 1351–1355.

[187] E. J. W. Verwey, K. F. Nielsen, *Phil. Mag.* **28** (1939) 435–436.

[188] D. L. Chapman, *Phil. Mag.* **25** (1913) 475.

[189] G. Gouy, *Compt. Rend. Acad. Sci.* **149** (1910) 654–657.

[190] C. Gavach, P. Seta, B. d'Epenoux, *J. Electroanal. Chem.* **83** (1977) 225–235.

[191] H. H. Girault, D. J. Schiffrin, *J. Electroanal. Chem.* **150** (1983) 43–49.

[192] Z. Samec, V. Mareček, D. Homolka, *J. Electroanal. Chem.* **187** (1985) 31–51.

[193] M. Faraday, *Philos. Trans* **147** (1857) 145–181.

[194] R. P. Andres, T. Bein, M. Dorogi, S. Feng, J. J. Henderson, C. P. Kubiak, W. Mahoney, R. G. Osifchin, R. Reifenberger, *Science* **272** (1996) 1323–1325.

[195] Galletto, P. F. Brevet, H. H. Girault, R. Antoine, M. Broyer, *J. Phys. Chem B* **103** (1999) 8706–8710.

[196] C. A. Mirkin, R. L. Letsinger, R. C. Mucic, J. J. Storhoff, *Nature* **382** (1996) 607–609.

[197] M. A. Hayat (Ed.), Colloidal Gold, Academic Press, San Diego, CA, 1991.

[198] J. S. Bradley, *in* Clusters and Colloids, G. Schmid (Ed.), VCH, Weinheim, 1994, pp. 459–544.

[199] E. Dujardin, S. Mann, L. B. Hsin, C. R. C. Wang, *Chem. Commun.* (2001) 1264–1265.

[200] M. Brust, M. Walker, D. Bethell, D. J. Schiffrin, R. Whyman, *J. Chem. Soc., Chem. Commun.* (1994) 801–802.

[201] J. Fink, C. J. Kiely, D. Bethell, D. J. Schiffrin, *Chem. Mater.* **10** (1998) 922–926.

[202] D. V. Leff, L. Brandt, J. R. Heath, *Langmuir* **12** (1996) 4723–4730.

[203] D. A. Handley, Colloid Gold: Principles, Methods and Applications, M. A. Hayat (Ed.).

[204] S. Chen, K. Kimura, *Langmuir* **15** (1999) 1075–1082.

[205] M. Brust, J. Fink, D. Bethell, D. J. Schiffrin, C. J. Kiely, *J. Chem. Soc., Chem. Commun.* (1995) 1655–1656.

[206] R. S. Ingram, M. J. Hostetler, R. W. Murray, *J. Am. Chem. Soc.* **119** (1997) 9175–9178.

[207] L. O. Brown, J. E. Hutchison, *J. Am. Chem. Soc.* **119** (1997) 3921–3926.

[208] R. S. Johnson, S. D. Evans, S. W. Mahon, A. Ulman, *Langmuir* **13** (1997) 51–57.

[209] S. Lee, V. Pérez-Luna, *Colloids Surf. B* **23** (2002) 95–114.

[210] Y. Shai, *Biochim. Biophys. Acta* **1462** (1999) 55–70.

[211] J. L. Thomas, D. A. Tirrel, *J. Controlled Release* **67** (2000) 203–209.

[212] W. Yu, M. Liu, H. Liu, X. Ma, Z. Liu, *J. Colloid Interface Sci.* **208** (1998) 439–444.

[213] C. Pan, K. Pelzer, K. Philippot, B. Chaudret, F. Dassenoy, P. Lecante, M.-J. Casanove, *J. Am. Chem. Soc.* **123** (2001) 7584–7593.

[214] G. Viau, R. Brayner, L. Poul, N. Chakroune, E. Lacaze, F. Fiévet-Vincent, F. Fiévet, *Chem. Mater.* **15** (2003) 486–494.

[215] J. Yang, J. Y. Lee, T. C. Deivaraj, H.-P. Too, *J. Colloid Interface Sci.* **271** (2004) 308–312.

[216] G. Decher, *Science* **277** (1997) 1232–1237.

[217] G. Decher, J. D. Hong, *Thin Solid Films* **210** (1992) 831–835.

[218] J. H. Fendler, *Chem. Mater.* **13** (2001) 3196–3210.

[219] Y. Cheng, M. Corn, *J. Phys. Chem.* **103** (1999) 8726–8731.

[220] M. Houska, E. Brynda, K. Bohatá, *J. Colloid Interface Sci.* **273** (2004) 140–147.

[221] C. J. Slevin, A. Mälkiä, P. Liljeroth, M. Toiminen, K. Kontturi, *Langmuir* **19** (2003) 1287–1294.

[222] A. Hugerth, L.-O. Sundelöf, *Langmuir* **16** (2000) 4940–4945.

[223] K. Kogej, E. Theunissen, H. Reynaers, *Langmuir* **18** (2002) 8799–8805.

[224] Y. Fu, H. Xu, S. Bai, D. Qiu, J. Sun, Z. Wang, X. Zhang, *Macromol. Rapid Commun.* **23** (2002) 256–259.

[225] P. Schuetz, F. Caruso, *Colloids Surf. A* **207** (2002) 33–40.

[226] J. F. Hicks, Y. Seok-Shon, R. W. Murray, *Langmuir* **18** (2002) 2288–2294.

[227] N. E. Cant, H.-L. Zhang, K. Critchley, T. A. Mykhalyk, G. R. Davies, S. D. Evans, *J. Phys. Chem. B* **107** (2003) 13557–13562.

[228] N. Ferreyra, L. Coche-Guérente, J. Fatisson, M. L. Teijelo, P. Labbé, *Chem. Commun.* (2003) 2056–2057.

[229] V. Ruiz, P. Liljeroth, B. M. Quinn, K. Kontturi, *Nano Lett.* **3** (2003) 1459–1462.

[230] S. Tian, J. Liu, T. Zhu, W. Knoll, *Chem. Commun.* (2003) 2738–2739.

[231] T. Sennerfors, G. Bogdanovic, F. Tiberg, *Langmuir* **18** (2002) 6410–6415.

[232] L. Krasemann, B. Tieke, *Langmuir* **16** (2000) 287–290.

[233] M. L. Bruening, D. M. Sullivan, *Chem. Eur. J.* **8** (2002) 3833–3837.

[234] A. A. Antipov, G. B. Sukhorukov, H. Möhwald, *Langmuir* **19** (2003) 2444–2448.

[235] C. Y. Gao, S. Leporatti, S. Moya, E. Donath, H. Möhwald, *Chem. Eur. J.* **9** (2003) 915–920.

[236] A. C. Templeton, W. P. Wuelfing, R. W. Murray, *Acc. Chem. Res.* **33** (2000) 27–36.

[237] J. H. Fendler (Ed.), Nanoparticles and Nanostructures Films: Preparation, Characterization and Applications, Wiley-VCH, Weinheim, 1998.

[238] M.-C. Daniel, D. Astruc, *Chem. Rev.* **104** (2004) 293–346.

[239] K. Uosaki, T. Kondo, M. Okamura, W. Song, *Faraday Discuss.* **121** (2002) 373–389.

[240] M. Chirea, V. García-Morales, J. A. Manzanares, C. Pereira, R. Gulaboski, F. Silva, *J. Phys. Chem. B* **109** (2005) 21808–21817.

[241] J. Zhao, C. R. Bradbury, S. Huclova, I. Potapova, M. Carrara, D. J. Fermín, *J. Phys. Chem. B* **109** (2005) 22985–22994.

[242] A. M. Yu, Z. J. Liang, J. H. Cho, F. Caruso, *Nano Lett.* **3** (2003) 1203–1207.

[243] X. Qiu, S. Leporatti, E. Donath, H. Möhwald, *Langmuir* **17** (2001) 5375–5380.

[244] A. G. Skirtach, C. Dejugnat, D. Braun, A. S. Susha, A. L. Rogach, W. J. Parak, H. Möhwald, G. B. Sukhorukov, *Nano Lett.* **5** (2005) 1371–1377.

[245] C. Mangeney, F. Ferrage, I. Aujard, V. Marchi-Artzner, L. Jullien, O. Ouari, E. D. Rékaï, A. Laschewsky, I. Vikholm, J. Sadowski, *J. Am. Chem. Soc.* **124** (2002) 5811–5821.

[246] I. Jelesarov, H. R. Bosshard, *J. Mol. Recognit.* **12** (1999) 3–18.

[247] J. Fanghänel, S. Wawra, C. Lucke, D. Wildemann, G. Fischer, *Anal. Chem.* **78** (2006) 4517–4523.

[248] J. E. Ladbury, *Thermochimica Acta* **380** (2001) 209–215.

[249] G. A. Holdgate, A. Tunnicliffe, W. H. Ward, S. A. Weston, G. Rosenbrock, P. T. Barth, I. W. Taylor, R. A. Pauptit, D. Timms, *Biochemistry* **36** (1997) 9663–9673.

[250] J. M. Sturtevant, *Proc. Natl. Acad. Sci. USA* **74** (1977) 2236–2240.

[251] R. S. Spolar, M. T. J. Record, *Science* **263** (1994) 777–784.

[252] P. R. Connelly, J. A. Thomson, *Proc. Natl. Acad. Sci. USA* **89** (1992) 4781–4785.

[253] J. E. Ladbury, *Chem. Biol.* **3** (1996) 973–980.

[254] P. R. Connelly, R. A. Aldape, F. J. Bruzzese, S. P. Chambers, M. J. Fitzgibbon, M. A. Fleming, S. Itoh, D. J. Livingston, M. A. Navia, J. A. Thomson, K. P. Wilson, *Proc. Natl. Acad. Sci. USA* **91** (1994) 1964–1968.

[255] R. Pignatello, V. D. Intravaia, G. Puglisi, *J. Colloid Interface Sci.* **299** (2006) 626–635.

[256] P. S. Charifson, L. M. Shewchuk, W. Rocque, C. W. Hummel, S. R. Jordan, C. Mohr, G. J. Pacofsky, M. R. Peel, M. Rodriguez, D. D. Sternbach, T. G. Consler, *Biochemistry* **36** (1997) 6283–6293.

[257] A. Ziegler, J. Seelig, *Biophys. J.* **86** (2004) 254–263.

[258] E. Gonçalves, E. Kitas, J. Seelig, *Biochemistry* **44** (2005) 2692–2702.

[259] E. Gonçalves, E. Kitas, J. Seelig, *Biochemistry* **45** (2006) 3086–3094.

[260] A. Z. X. Blatter, A. Seelig, J. Seelig, *Bichemistry* **42** (2002) 9185–9194.

[261] C. P. Swaminathan, A. Nandi, S. S. Visweswariah, A. Surolia, *J. Biol. Chem.* **274** (1999) 31272–31278.

[262] M. Banerjee, A. Poddar, G. Mitra, A. Surolia, T. Owa, B. Bhattacharyya, *J. Med. Chem.* **48** (2005) 547–555.

[263] S. Sharma, S. Bharadwaj, A. Surolia, S. K. Podder, *Biochem. J.* **333** (1998) 539–542.

[264] K. de Meijere, G. Brezesinski, H. Möhwald, *Langmuir* **14** (1998) 4204–4209.

[265] O. Zschörnig, W. Richter, G. Paasche, K. Arnold, *Colloid Polym. Sci.* **278** (2000) 637–646.

[266] G. Cevc, Phospholipids Handbook, Marcel Dekker, New York, 1993.

[267] F. Cabassi, B. Casu, A. Perlin, *Carbohydr. Res.* **63** (1978) 1–11.

[268] Z. Kozarac, B. Ćosović, D. Möbius, M. Dobrić, *J. Colloid Interface Sci.* **226** (2000) 210–217.

[269] T. Kakiuchi, M. Senda, *Collect. Czech. Chem. Commun.* **56** (1991) 112–129.

ISBN 978-951-22-8888-5
ISBN 978-951-22-8889-2 (PDF)
ISSN 1795-2239
ISSN 1795-4584 (PDF)